

INVESTIGATION OF METALLOANTIBODY CATALYZED ESTER
HYDROLYSIS

by
MAUREEN F. BURKART

A DISSERTATION PRESENTED TO THE GRADUATE SCHOOL OF THE
UNIVERSITY OF FLORIDA IN PARTIAL FULFILLMENT OF THE
REQUIREMENTS FOR THE DEGREE OF DOCTOR OF PHILOSOPHY

UNIVERSITY OF FLORIDA
1995

UNIVERSITY OF FLORIDA LIBRARIES

To my Father

ACKNOWLEDGEMENTS

Earnest appreciation goes to Dr. Richardson for his ideas and thoughts and advice, and thanks to all the members of my doctoral committee for their generous assistance throughout these past few years. I am grateful for the support of all members of the Richardson group, past and present, who not only made the laboratory environment a pleasant one, but also taught me a great deal about a great many things. Much gratitude goes to all members of the Hybridoma Core Laboratory for their abundant help, understanding, and hard work. Appreciation goes to Dr. Schanze and his group for the use of their spectrophotometer. I thank Dr. Sisler for his gracious support and advice. I am grateful to many others - Jeni, Brae, Dione, Linda, Scherwin, Jerrold, Lucia - who have always been there when I really needed them. I must also express enormous appreciation to my father, Oswald Burkart, for his constant support and love and faith in me; without him, I never would have made it this far.

This research project was made possible through the generous financial support of the National Institutes of Health and the University of Florida.

TABLE OF CONTENTS

ACKNOWLEDGEMENTS.....	iii
LIST OF FIGURES.....	vi
ABSTRACT.....	ix
CHAPTERS	
1 INTRODUCTION.....	1
2 TRANSITION STATE STABILIZATION APPROACH: SYNTHESIS OF A HAPTEN.....	14
Introduction.....	14
Synthetic Plan.....	20
Results and Discussion.....	21
Experimental Methods.....	33
Conclusions.....	35
3 SEMI-SYNTHETIC PROCEDURE: PREPARATION OF A METALLOANTIBODY.....	37
Introduction.....	37
Synthetic Plan.....	40
Results and Discussion.....	43
Experimental Methods.....	52
Conclusions.....	59
4 PRELIMINARY KINETIC STUDIES ON METALLOANTIBODY CATALYZED HYDROLYSIS OF ESTERS.....	61
Introduction.....	61
Results and Discussion.....	64
Experimental Methods.....	90
Conclusions.....	93
5 CONCLUSION.....	96

APPENDICES

A ATTEMPTED FUNCTIONALIZATION OF 2,2'- DIPYRIDYLAMINE	100
B PROTON NMR SPECTRUM OF 4 IN ACETONE-d ₆	102
C CARBON NMR SPECTRUM OF 4 IN ACETONE-d ₆	104
D PROTON NMR SPECTRUM OF 6 IN DMSO-d ₆	106
E DERIVATION OF THE EXPRESSION $\ln(\text{Pr} - x) = -k_{\text{obs}}t + \ln(\text{Pr})$...	108
REFERENCES.....	109
BIOGRAPHICAL SKETCH.....	114

LIST OF FIGURES

Figure	Page
1.1 Energy profile of a chemical reaction.....	3
1.2 Abzyme catalyzed carbonate hydrolysis.....	5
1.3 Abzyme catalyzed ester hydrolysis.....	6
1.4 Preparation of a semi-synthetic abzyme.	8
1.5 Coumarin ester.	9
1.6 Hydrolysis catalyst.	11
1.7 Copper complex-catalyzed hydrolysis of methyl acetate.	12
2.1 Ethyl acetate hydrolysis.	16
2.2 Proposed transition state for ethyl acetate hydrolysis and its model.	17
2.3 Energy diagram.	19
2.4 Scheme for synthesis of hapten.	22
2.5 Szabo and Menn procedure.	23
2.6 Potential transition state analogues.	26
2.7 Dipyriddy ligand functionalization.	27
2.8 Cofactor model preparation.	31
2.9 Formation of hapten.	32
3.1 Preparation of a semi-synthetic abzyme.	38
3.2 (N-2,4-Dinitrophenyl)-2-aminoethyl 4-oxobutyl disulfide, Linker.	41

Figure	Page
3.3 Scheme for preparation of a metalloantibody.	44
3.4 MOPC-315 Fab 4-10% SDS-PAGE gel electrophoresis results.	45
3.5 Elution peak of MOPC-315 Sephacryl S-100-HR FPLC.	47
3.6 Outline for synthesis of the linker.	49
3.7 Functionalization of 2,2'-dipyridylamine.	50
3.8 Semi-synthetic metallantibody preparation.	53
4.1 Hydrolysis of 2,4-dinitrobenzoic acid, 7-hydroxycoumarin ester.	62
4.2 Hydrolysis of 2,4-dinitrophenyl acetate.	63
4.3 Plot of fluorescent intensity versus time (s) for hydrolysis of 2,4-dinitrobenzoic acid, 7-hydroxycoumarin ester.	66
4.4 Hydrolysis of <i>p</i> -nitrophenyl acetate.	68
4.5 Plot of A_{417} versus time (min) for $\{(2,2'\text{-dipyridylamine})\text{Cu}(\text{OH}_2)_2\}^{2+}$ catalyzed hydrolysis of <i>p</i> -nitrophenyl acetate.	69
4.6 Plot of A_{417} versus concentration of <i>p</i> -nitrophenol.	70
4.7 Plot of $\ln(C_\infty - C_t)$ versus time (min) for the initial rate of $\{(2,2'\text{-dipyridylamine})\text{Cu}(\text{OH}_2)_2\}^{2+}$ catalyzed hydrolysis of <i>p</i> -nitrophenyl acetate.	72
4.8 Plot of A_{410} versus concentration of 2,4-dinitrophenol.	74
4.9 Plot of A_{410} versus time (s) for $\{(2,2'\text{-dipyridylamine})\text{Cu}(\text{OH}_2)_2\}^{2+}$ catalyzed hydrolysis of 2,4-dinitrophenyl acetate.	75
4.10 Plot of $\ln(C_\infty - C_t)$ versus time (s) for the initial rate of $\{(2,2'\text{-dipyridylamine})\text{Cu}(\text{OH}_2)_2\}^{2+}$ catalyzed hydrolysis of 2,4-dinitrophenyl acetate.	76
4.11 Plot of $\ln(C_\infty - C_t)$ versus time (s) for $\{(2,2'\text{-dipyridylamine})\text{-Cu}(\text{OH}_2)_2\}^{2+}$ catalyzed hydrolysis of 2,4-dinitrophenyl acetate.	77

Figure		Page
4.12	Plot of A_{410} versus time (s) for hydrolysis of 2,4-dinitrophenyl acetate in the presence of 0.1 mM 2,4-dinitrophenol.	79
4.13	Plot of A_{410} versus time (s) for dipyridylamine-functionalized Fab catalyzed hydrolysis of 2,4-dinitrophenyl acetate.	82
4.14	Plot of A_{410} versus time (s) for hydrolysis of 2,4-dinitrophenyl acetate in the presence of pH 4.9 metallated dipyridylamine-functionalized Fab.	84
4.15	Plot of $\ln(C_{\infty} - C_t)$ versus time (s) for dipyridylamine-functionalized Fab catalyzed hydrolysis of 2,4-dinitrophenyl acetate.	85
4.16	EPR spectra for copper(II) nitrate (top), 1 (middle), and 1 with excess dipyridylamine (bottom).	88
4.17	EPR spectra for 1 at various pH values.	89

Abstract of Dissertation Presented to the Graduate School of the University of Florida
in Partial Fulfillment of the Requirements for the Degree of Doctor of Philosophy

INVESTIGATION OF METALLOANTIBODY CATALYZED ESTER
HYDROLYSIS

By

Maureen F. Burkart

December, 1995

Chairperson: David E. Richardson

Major Department: Chemistry

In recent years, antibodies have been used as catalysts for a variety of chemical reactions. Interest in catalytic antibodies, also known as abzymes, stems from their potential use as synthetic enzymes. The steric and electronic complementarity between the binding site of an antibody and its antigen has been compared to the complementarity that exists between the active site of an enzyme and its substrate. Antibody-antigen interactions tend to be strong and specific, two properties that can be exploited to create an efficient catalyst.

The present research was focused on expanding the applicability of abzymes by incorporation of a metal complex cofactor. Metalloantibodies that catalyze hydrolysis of esters and amides are of particular interest because of the extensive biological, medical, and industrial applications of such catalysts. The complex {(2,2'-

dipyridylamine) $\text{Cu}(\text{OH}_2)_2\}^{2+}$ was chosen for incorporation into an antibody as it is an efficient catalyst for hydrolysis of esters and amides.

One approach taken toward development of metalloabzymes has been transition state stabilization. This approach involves synthesis of an antigen that models the rate controlling, high energy transition state/intermediate of a reaction and use of this antigen to elicit antibodies. The resulting antibodies, by virtue of their affinity for the high energy species, should cause rate acceleration through binding. The synthesis of an antigen designed to elicit antibodies that function as hydrolysis catalysts in conjunction with $\{(2,2'\text{-dipyridylamine})\text{Cu}(\text{OH}_2)_2\}^{2+}$ was attempted.

Another method for metalloabzyme development that has been investigated is the semi-synthetic procedure. The procedure entails introduction of a catalytic group directly into the binding site of an antibody. In this study, antibody fragments with high affinity for dinitrophenyl groups were coupled to $\{(2,2'\text{-dipyridylamine})\text{Cu}(\text{OH}_2)_2\}^{2+}$. The antibodies should cause catalysis by bringing the substrate and catalyst into close proximity. The ability of the semi-synthetic metalloantibodies to catalyze hydrolysis of 2,4-dinitrophenyl acetate was examined through kinetic studies.

CHAPTER 1 INTRODUCTION

Scientists have long been interested in mimicking nature's catalysts, the enzymes. Enzymes are highly efficient, stereospecific catalysts that function under mild conditions. Synthetic catalysts with the properties of enzymes could have extensive biological, medical, and industrial applications.¹

Much of the work towards development of artificial enzymes has been in the area of biomimetic chemistry. Chemical models designed to imitate some aspect of enzyme catalysis are synthesized and studied.² Difficulties in this method arise when one must introduce the complexities of a large protein molecule into the chemical model; synthetic capabilities become the limiting factors. Another approach toward the problem is to begin with a substance that has the same level of complexity as an enzyme and manipulate it so that it will act as a catalyst. This has been achieved through modification of proteins and existing enzymes, i.e. protein engineering.³

The use of antibodies as precursors to artificial enzymes has an important benefit over these other methods since the difficult task of engineering substrate specificity is eliminated.⁴ The basis for the use of antibodies as catalysts was pointed out many years ago when Pauling proposed that each enzyme evolved so that the active site is complementary to the rate-determining transition state of the reaction it catalyzes.⁵ The enzyme binds selectively to the transition state, thereby stabilizing it

and lowering the activation energy for the reaction. In this way, the reaction rate is enhanced. Further, Pauling suggested that the major difference between enzymes and antibodies is that enzymes are complementary to and thus bind the transition state, whereas antibodies bind a ground state molecule.⁵ This proposal led Jencks to propose that an enzyme could be prepared by obtaining an antibody specific for a haptenic group which resembles the transition state of a given reaction.⁶ Jencks offered a way to exploit the huge diversity of the immune response and the specificity of the antibody-antigen interaction to create a synthetic enzyme.

The ability to produce large amounts of monoclonal antibodies *in vitro*, a result of the development of hybridoma technology,⁷ led to the realization of Jencks' suggestion. As a result of this success, several different general strategies toward development of catalytic antibodies have arisen. Two of these strategies are of interest to this work, (1) the transition state stabilization approach and (2) the semi-synthetic procedure. The first approach is based on Jencks' original idea about the use of antibodies as enzymes. Enzymes have evolved such that the active site stabilizes the transition state relative to reactants or products. Thus, antibodies are developed to stabilize high-energy reaction intermediates. This is accomplished through synthesis of a species that models the transition state of the desired reaction followed by use of that species as a hapten to elicit antibodies. The resulting antibodies are complementary to the transition state and force bound substrate molecules to resemble that high-energy species. The binding lowers the free energy of activation for reaction and increases the reaction rate (Figure 1.1). Transition state analogues that are used to elicit catalytic

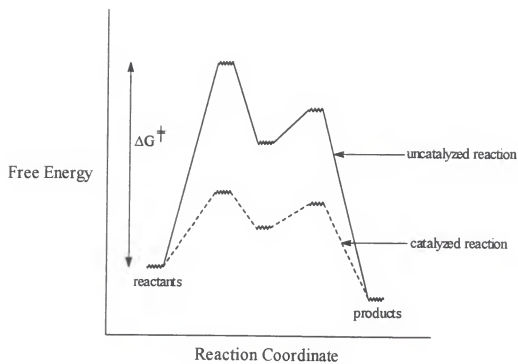


Figure 1.1
Energy profile of a chemical reaction

antibodies are often inhibitors for analogous enzymes because they are structurally and electronically similar to the high energy species that the enzyme binds and stabilizes.⁸

The first antibody-catalyzed reactions were simple hydrolytic ones. The transition state for these reactions is considerably different from the substrate in terms of geometric and electronic properties, e.g., the transition state is tetrahedral and negatively charged whereas the substrate is planar and neutral. This structural difference suggests that eliciting antibodies that preferentially bind the transition state is feasible.⁴ In 1986, Pollack and coworkers reported that antibodies raised to a tetrahedral, negatively charged phosphate transition state analogue could selectively catalyze the hydrolysis of carbonates (Figure 1.2).⁹ The rate enhancement was 770 above the uncatalyzed reaction. At the same time, Tramontano and coworkers described antibodies that could catalyze the hydrolysis of esters; these antibodies had been raised against a phosphonate transition state analogue (Figure 1.3).¹⁰ Rate enhancement was on the order of 960. These are the first published examples of the development and generation of a catalytic antibody, or abzyme.

The semi-synthetic procedure involves introduction of a catalytic group into an antibody with the desired specificity. A catalyst is covalently linked to the antibody molecule in close proximity to the substrate binding site. The resulting antibody is complementary to and binds the substrate, and this binding brings the substrate close to the catalyst so that rate enhancement can occur. Pollack et al. have developed a general procedure for selectively introducing a catalyst, or other reactive species, into the binding site of the MOPC-315 monoclonal antibody.¹¹

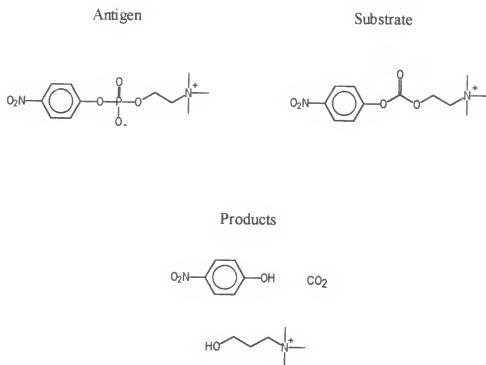


Figure 1.2
Abzyme catalyzed carbonate hydrolysis

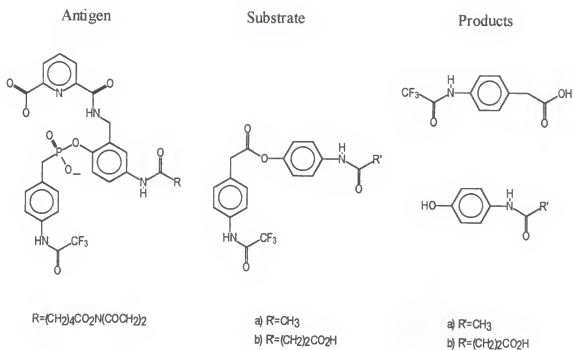


Figure 1.3
Abzyme catalyzed ester hydrolysis

Immunoglobulin A MOPC-315 is a well-studied, well-characterized antibody.¹² Its binding specificity is for molecules that contain 2,4-dinitrophenyl groups; association constants range from 5×10^4 to $1 \times 10^6 \text{ M}^{-1}$.¹³ The X-ray crystal structure of MOPC-315 is not yet known; however, the antigen binding site has been characterized by spectroscopic methods (ultraviolet, fluorometry, nuclear magnetic resonance), chemical modification, and amino acid sequencing of the variable region. Further, affinity-labeling studies have revealed the location of reactive amino acid side chains in the region around the binding site.¹⁴ One of these amino acid side chains, that of Lys52H, has been selectively modified with a thiol through the use of cleavable affinity labels. This modification has made it possible to attach a catalytic group into the binding site of MOPC-315. Pollack et al. attached an imidazole group to the MOPC-315 binding site (Figure 1.4).¹¹ The resulting abzyme causes a rate acceleration of $(1.1 \pm 0.2) \times 10^3$ times that of the 4-methylimidazole catalyzed reaction for hydrolysis of the coumarin ester shown in Figure 1.5. This enhancement is comparable to that observed for the transition state stabilization method.

In the subsequent years, antibodies have been produced that catalyze a vast number of chemical reactions.^{1,4} The diversity in these abzyme-catalyzed reactions is impressive, ranging from the acyl transfer reactions to Diels-Alder and redox transformations. In terms of specificity, the abzyme-catalyzed reactions are similar to or, in some cases, surpass enzyme-catalyzed reactions. However, when comparing rate enhancements, enzymatic reactions are still much faster. Abzymes achieve rate increases on the order of only 10^3 to 10^6 ,^{1,4} compared to 10^9 for some enzymes.¹⁵

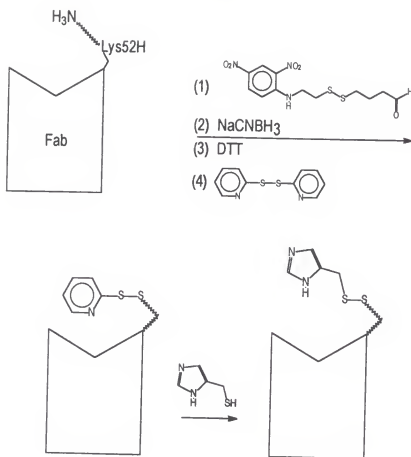


Figure 1.4
Preparation of a semi-synthetic abzyme

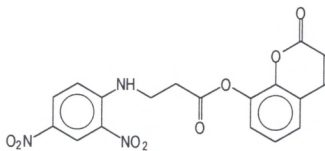


Figure 1.5
Coumarin ester

The next level in the evolution of abzymes is incorporation of a metal complex cofactor. Many naturally occurring enzymes work in association with a metal ion in the active site. Examples include carboxypeptidase A, carbonic anhydrase, alkaline phosphatase, and several dipeptidases.¹⁵ Incorporation of metal complexes should increase the scope of antibody catalysis as well as provide insight into metalloenzyme catalysis.

Antibodies that catalyze hydrolysis of carboxylate esters, phosphate esters, and amides are of particular interest. The potential applications of tailor-made hydrolytic catalysts, including selective cleavage of physiological targets, provide a compelling reason to pursue development of hydrolytic catalytic antibodies. In order to develop hydrolytic metalloantibodies, an appropriate metal complex must be investigated. A copper complex studied by Chin and coworkers has been found to catalyze hydrolysis of esters and amides efficiently.¹⁶ The complex shown in Figure 1.6, $\{(2,2'$ -dipyridylamine) $\text{Cu}(\text{OH}_2)_2\}^{2+}$ (**1**), catalyzes the hydrolysis of methyl acetate (rate enhancement of 2.4×10^6) and *p*-nitrophenyl acetate (rate enhancement 2.7×10^5). It is interesting that the complex gives greater rate acceleration for the unactivated ester than for the activated one since many simple hydrolysis catalysts are more efficient with activated species.¹⁷ It has been proposed that the mechanism of the metal ion promoted hydrolysis involves Lewis acid action by the metal ion to activate both the substrate and a water molecule. This sort of mechanism would imply a transition state in which the copper ion is coordinated to an oxygen atom within the substrate and another oxygen atom from a water molecule (Figure 1.7). The simplicity and

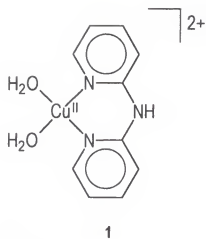


Figure 1.6
Hydrolysis catalyst

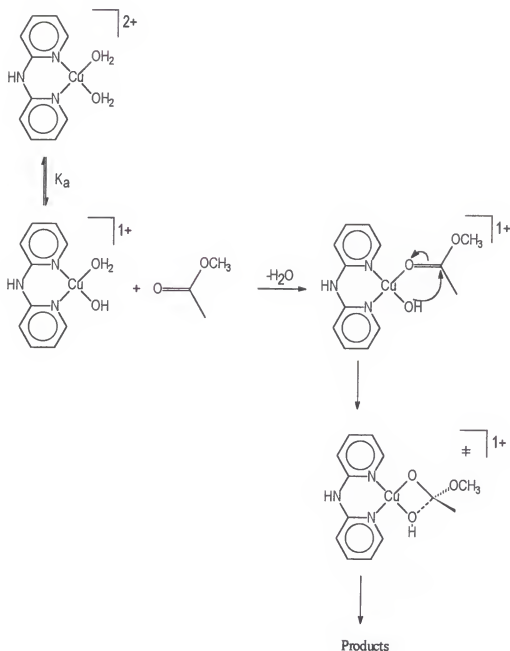


Figure 1.7
Copper complex-catalyzed hydrolysis of methyl acetate

favorable activity of **1** make it a desirable candidate for incorporation into a metalloabzyme.

The main goal of this work has been to develop metalloabzymes for ester hydrolysis, that is, to produce antibodies that will catalyze the hydrolysis of esters in conjunction with a metal complex cofactor. To do this, both the transition state stabilization approach and the semi-synthetic procedure have been employed. The details of preparation of abzymes that work in combination with the copper (II) dipyritylamine complex will be discussed.

CHAPTER 2 TRANSITION STATE STABILIZATION APPROACH: SYNTHESIS OF A HAPTEN

Introduction

This study was designed to expand the transition state stabilization approach toward development of catalytic antibodies to include a metal complex cofactor. This goal could be accomplished by eliciting antibodies against a transition state analogue that contains a metal complex. Antibodies elicited against metal complexes have been reported. Schwabacher and coworkers raised monoclonal antibodies against metalloporphyrin complexes,¹⁸ and Reardan and coworkers prepared monoclonal antibodies using an indium-EDTA chelate.¹⁹ These studies show that an antibody may be induced to bind a metal complex in the antigen combining site.

In an attempt to produce cofactor-assisted peptide hydrolysis catalysts, Iverson and Lerner generated monoclonal antibodies specific for a metal-substrate complex.²⁰ The complex consists of a kinetically inert cobalt moiety connected to a peptide chain. Antibodies in the presence of metal cofactor were found to exhibit catalysis for hydrolysis of substrates that bear close resemblance to the hapten; a catalytic rate constant of 6×10^{-4} per second was detected for these substrates. These antibodies may be considered metalloabzymes as the active abzyme requires binding of a metal cofactor. However, the study is illogical in certain ways. For instance, an antibody

specific for the substrate of a reaction will not necessarily bind the high energy transition state. A hapten containing a substance resembling the transition state would be a more reasonable choice for eliciting a catalytic antibody because the basis for rate enhancement in this approach is stabilization of the transition state relative to reactants and products. Another interesting point is that the bond cleaved within the tetrapeptide substrates upon metalloabzyme catalyzed hydrolysis is not the bond closest to the metal complex. It would seem logical for the metal complex to have an effect on the bond to which it is closest. As noted by the authors, the mechanism by which this metalloabzyme catalyzes hydrolysis is not clear.

In order to incorporate a metal complex cofactor into the transition state stabilization approach, a hapten that models the transition state for a metal complex catalyzed reaction must be synthesized. An example of a reaction catalyzed by Chin's copper complex is shown in Figure 2.1. The objective of this work was to synthesize a hapten that models the transition state for this copper complex catalyzed reaction and use that hapten to elicit antibodies. The resulting antibodies should be capable of binding the transition state and, therefore, should act as catalysts in the presence of the copper complex.

A proposed transition state for the copper complex catalyzed hydrolysis of ethyl acetate as well as a complex fashioned to model it are shown in Figure 2.2. The model was designed as a stable compound to mimic the structural features of the transition state, most notably the square planar geometry about the metal and the tetrahedral geometry about the central carbon of the ester. The carbon chain



Figure 2.1
Ethyl acetate hydrolysis

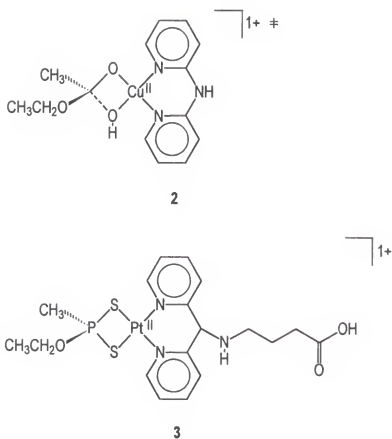


Figure 2.2
Proposed transition state for ethyl acetate hydrolysis and its model

extending from the dipyridyl ligand provides a means to attach the model to a carrier protein; a substance with this capability is said to be functionalized for bioconjugation. This chapter describes the attempted synthesis of this unique hapten.

It should be noted that the transition state(s) of a reaction is a high energy, nonisolable species, and so its true structure can never be known for certain. The proposed structure shown in Figure 2.2 may not represent an exact model for the transition state of the copper complex catalyzed reaction. However, this does not mean that antibodies specific for the complex designed to model it will be inactive. It can be said that the structure probably mimics some high energy species along the reaction pathway and that this species resembles the transition state of the reaction more than it resembles the reactants or products. All substances will be stabilized through binding with the antibody, but some will be stabilized more than others. The substances that will be stabilized the most are those that contain the highest degree of complementarity with the binding site of the antibody. In Figure 2.3, transition state A represents the activated complex that leads to formation of the tetrahedral intermediate. Transition state B represents the activated complex involved in proton transfer. Since the proposed structure resembles a transition state more than the reactants, and the antibody will be most specific for that structure, then a transition state will be stabilized relative to the reactants. In light of this, use of the term "transition state analogue" should not be taken literally. "Transition state analogue" refers to a structural mimic of some high energy species along the reaction pathway.

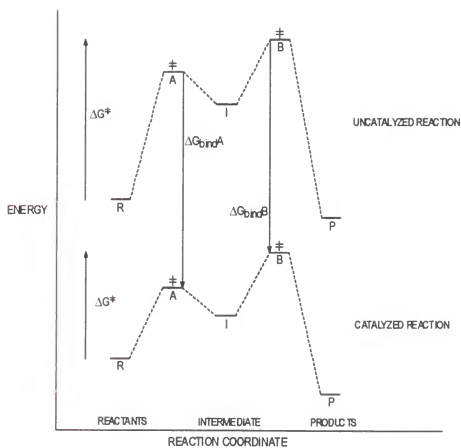


Figure 2.3
Energy diagram

Synthetic Plan

The first step in preparation of the hapten was synthesis of a complex to model the proposed transition state for ester hydrolysis. Phosphonate esters have been used extensively as transition state analogues for the production of hydrolytic catalytic antibodies^{1,4} and were considered promising candidates. Also, techniques for the preparation of phosphonate esters and their thiol analogues have been established due to their use as insecticides and insecticidal precursors.²¹ A phosphonodithioic acid was selected as an appropriate transition state analogue for a reason that will become clear.

The next stage in generation of the hapten was preparation of a functionalized cofactor model complex. Reductive amination of di-2-pyridyl ketone was chosen as a route to a suitable functionalized dipyridyl ligand. Attempts were made to functionalize 2,2'-dipyridylamine also, but the substance proved to be unreactive with the particular methods pursued (Appendix A). The functionalized ligand was used in the synthesis of the cofactor model complex. It was necessary for this model complex to retain the overall structure of the cofactor, i.e. square planar geometry, while remaining inactive as a hydrolysis catalyst. A platinum complex was perceived to be consistent with these requirements. Further, platinum-dipyridyl complexes have been well characterized, and their syntheses are straightforward.²²

The final stage in the synthetic scheme was reaction of the ester hydrolysis transition state analogue with the platinum-dipyridyl complex to form a complete, conjugatable hapten. Platinum exhibits a much stronger interaction with sulfur than

with oxygen, thus the placement of sulfur groups on the transition state analogue was required. With this requirement satisfied through the use of a phosphonodithioic acid, reaction between the dithiophosphonate ester and the functionalized platinum complex was anticipated to produce the desired product. The overall synthetic plan is shown in Figure 2.4.

Results and Discussion

Preparation of the Ester Hydrolysis Transition State Analogue

The sodium salt of *O*-ethylmethylphosphonodithioic acid was prepared according to a method established by Szabo and Menn (Figure 2.5).²³ Isolation of **4** was accomplished in two different ways. The procedure employed by Szabo and Menn involved protonation to form the phosphonodithioic acid, extraction into diethyl ether, and vacuum distillation to give the pure acid. For the second method, the product was maintained in the salt form, and upon extraction with diethyl ether, it remained in the aqueous layer. Removal of the solvent afforded pure sodium *O*-ethylmethylphosphonodithioate. The second method proved to be more desirable because it supplied a higher yield of product.

Sodium *O*-ethylmethylphosphonodithioate was characterized by using ¹H and ¹³C nuclear magnetic resonance spectroscopy. The structure of the substance indicates that it could be a strong inhibitor of acetylcholinesterase and thus a strong toxin; exposure to it should be limited.

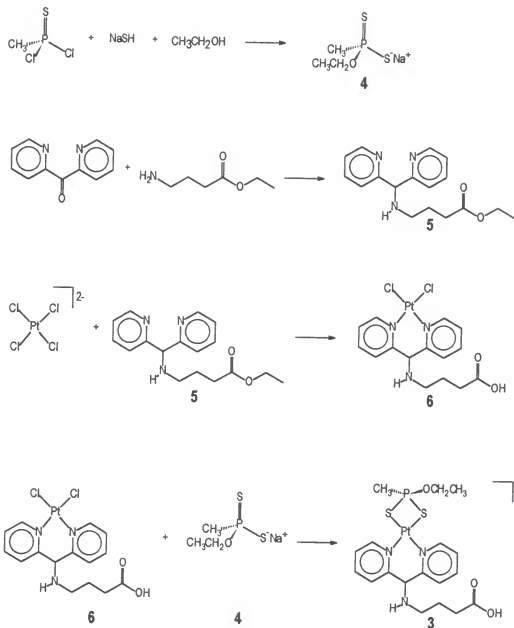


Figure 2.4
Scheme for synthesis of hapten

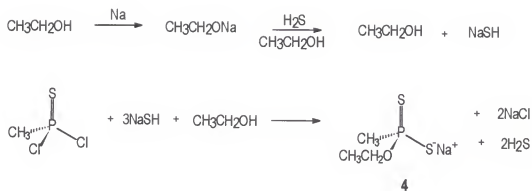


Figure 2.5
Szabo and Menn procedure

Considering the ^1H NMR spectrum of **4** in acetone- d_6 (Appendix B), it appears that phosphorous couples with protons two and three bonds away. The doublet at $\delta = 1.83$ ppm with $J = 15.0$ Hz corresponds to protons in the methyl group directly attached to the phosphorous. These protons are close to the phosphorous, and therefore their signal is split to a large extent. The methylene protons also couple with phosphorous, although the interaction is not as strong because the protons are three bonds away. The doublet of quartets at $\delta = 3.92$ ppm corresponds to these protons. Coupling constants indicate that the phosphorous-proton interaction is larger than the proton-proton interaction: $J_{\text{P-H}} = 9.0$ Hz, $J_{\text{H-H}} = 7.5$ Hz. The ethoxy group methyl protons are not affected by phosphorous; these protons correspond to the upfield triplet ($\delta = 1.15$ ppm, $J = 7.5$ Hz).

The ^{13}C NMR spectrum of **4** in acetone- d_6 indicates that phosphorous couples with carbon atoms one, two, and three bonds distant (Appendix C). As expected, the greatest interaction occurs with the carbon directly attached to the phosphorous ($\delta = 32.8$ ppm, $J = 330$ Hz). The influence of phosphorous on the ethoxy carbons is equivalent. The signal at $\delta = 57.6$ ppm corresponding to the methylene carbon and the signal at $\delta = 15.9$ ppm corresponding to the methyl carbon are both split to the same extent ($J = 30$ Hz).

Investigation of Other Potential Analogues

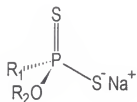
Use of sodium *O*-ethylmethylphosphonodithioate as a transition state analogue requires that the substrate for the corresponding hydrolysis reaction be ethyl acetate. It would be of interest to use other substrates as well. For instance, substrates with

bulkier groups should lead to stronger interaction with the abzyme. With this in mind, attempts were made to synthesize other phosphonodithioic acid salts in a manner similar to the preparation of **4**. Specifically, syntheses of phosphonodithioic acid salts **7-10**, Figure 2.6, were investigated. None of these species were isolated. In the case of **7**, the *p*-nitrophenol was unreactive most likely because it would not dissolve in a suitable, inert solvent. Use of neopentyl alcohol was likewise unsuccessful; the bulky group proved too sterically hindered to react. Reaction did occur for the *O*-ethylphenyl and *O*-benzylmethyl species, but the products were not as expected. NMR data indicate that an ethoxy group replaces one of the sulfurs to give *O,O*-diethylphenylphosphonothioic acid instead of *O*-ethylphenylphosphonodithioic acid. The analogous reaction occurred for the *O*-benzyl species. The reasons for these results are not clear.

Functionalization of the Dipyridyl Ligand

Functionalization of di-2-pyridyl ketone was accomplished via reductive amination. Di-2-pyridyl ketone, sodium cyanoborohydride, and an excess of ethyl 4-aminobutyrate hydrochloride were reacted in methanol to afford the crude product ethyl 5-amino-6-(2,2'-dipyridyl)hexanoate (**5**) (Figure 2.7). This preparation was based on a similar method described by Borch, Bernstein, and Durst.²⁴

Purification of **5** is not trivial. Extraction of the acidified reaction solution with diethyl ether serves to remove the excess ethyl 4-aminobutyrate starting material; the product remains in the aqueous layer. Extraction of basic aqueous layer with diethyl ether separates the product from the other reactants. Di-2-pyridyl ketone and sodium



7 $\text{R}_1 = \text{C}_6\text{H}_5$, $\text{R}_2 = p\text{-NO}_2\text{C}_6\text{H}_4$

8 $\text{R}_1 = \text{C}_6\text{H}_5$, $\text{R}_2 = \text{CH}_3\text{CH}_2$

9 $\text{R}_1 = \text{CH}_3$, $\text{R}_2 = \text{C}_6\text{H}_5\text{CH}_2$

10 $\text{R}_1 = \text{CH}_3$, $\text{R}_2 = (\text{CH}_3)_3\text{CCH}_2$

Figure 2.6
Potential transition state analogues

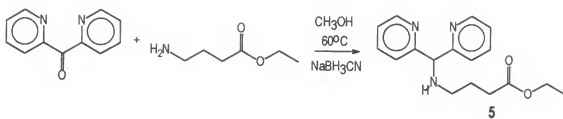


Figure 2.7
Dipyridyl ligand functionalization

cyanoborohydride remain in the aqueous layer, and **5** goes into the ether layer. The side-products are then removed via a chromatography series. A silica 60 Å column removes aliphatic impurities, and an alumina adsorption column removes aromatic impurities. The product is luminescent, so its progress on the column is easily monitored using a UV lamp. It is often necessary to repeat the chromatography series several times before a pure sample is obtained, and it is possible that loss on the columns contributes to the low yield.

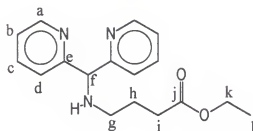
^1H and ^{13}C NMR spectroscopy were used to characterize ethyl 5-amino-6,6-(2,2'-dipyridyl)hexanoate. Table 2.1 lists the peak assignments. The NMR results are consistent with the predicted structure of the product.

Ethyl 5-amino-6,6-(2,2'-dipyridyl)hexanoate is apparently unstable under atmospheric conditions. It was necessary to store the functionalized ligand in the absence of light at 4°C because of decomposition. Under these conditions, NMR data indicated breakdown in the product after around seven days.

Preparation of the Cofactor Model Complex

It was anticipated that the platinum complex could be synthesized simply by allowing **5** to react with potassium tetrachloroplatinate (II) in water under reflux conditions; the neutral complex was expected to precipitate from the solution. Other platinum complexes, including dichloro-(2,2'-dipyridylamine)platinum (II) and dichloro-(di-2-pyridyl ketone)platinum (II), had been prepared in this exact manner. However, when this method was attempted, the result was a mixture of non-identifiable substances. This problem was apparently caused by the amine functionality

Table 2.1 NMR Data for Ethyl 5-amino-6,6-(2,2'-dipyridyl)hexanoate



Position	^1H δ , ppm/Multiplicity	$J_{\text{H-H}}$, Hz	^{13}C δ , ppm
a	8.49 d	8.1	160.7
b	7.76 t	8.1	148.5
c	7.25 t	6.0	122.4
d	7.50 d	7.5	122.5
e	-----	-----	137.1
f	5.19 s	-----	68.7
g	2.57 t	7.0	46.5
h	1.84 qn	7.8	24.7
i	2.36 t	7.2	31.5
j	-----	-----	173.7
k	4.06 q	7.5	60.0
l	1.19 t	6.6	13.1

in the ligand; the amine nitrogen competes with the pyridyl nitrogens for coordination to platinum. The reaction was repeated at $\text{pH} < 2$; under this condition, the amine nitrogen remained protonated and did not interfere. However, the acidic solution caused cleavage of the ester. The product **6** precipitated out of solution as a yellow solid. Figure 2.8 shows the reaction under the favorable reaction conditions.

Proton NMR data indicate that coordination of **5** to platinum causes a downfield shift for aromatic ligand protons (Appendix D). This is consistent with previous NMR studies involving platinum complexes.²⁵ Side bands from ^{195}Pt are present, although they are very weak, and the peaks for the aliphatic protons have undergone a dramatic broadening.

Reaction of Sodium *O*-ethyl-methylphosphonodithioate (**4**) with [5-Amino-6,6-(2,2'-dipyridyl)hexanoic acid]-dichloroplatinum (II) (**6**) to form the Hapten

In an attempt to produce the complete, conjugatable hapten, excess sodium *O*-ethylmethylphosphonodithioate was allowed to react with [5-Amino-6,6-(2,2'-dipyridyl)hexanoic acid]-dichloroplatinum (II) (Figure 2.9). Dimethyl sulfoxide- d_6 was used as the solvent so that reaction progress could be followed by ^1H NMR spectroscopy. Data indicate that the desired product is not formed. It appears that the excess of **4** leads to displacement of the dipyridyl ligand on platinum. The result is a mixture of platinum-*O*-ethylmethylphosphonodithioate complexes, possibly including polymers, and free dipyridyl ligand. This is not surprising considering the strong interaction that exists between platinum and sulfur. The reaction was run using stoichiometric ratios; again, a mixture was obtained. It is unclear whether or not the

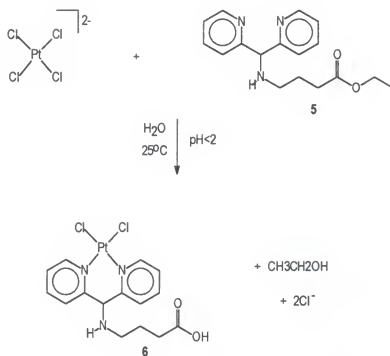


Figure 2.8
Cofactor model preparation

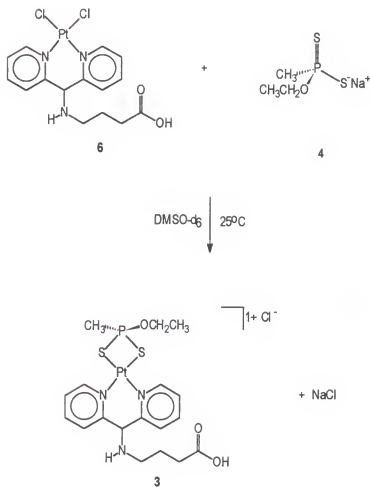


Figure 2.9
Formation of haptene

desired product is present. Purification using cation exchange chromatography was pursued, but this was not successful. The reaction was run in different solvents including DMF, acetone, and ethyl formate; still, a mixture was obtained. Lowering the temperature did not appear to improve the results.

Experimental Methods

General Procedures

Proton NMR and ^{13}C NMR spectra were recorded at 300 MHz on a General Electric QE-300 spectrometer. Chemical shifts are reported in parts per million; the residual solvent peak was used as an internal standard. Elemental analysis ($\text{C}, \text{H}, \text{N}$) was performed by the University of Florida Department of Chemistry Analytical Services. Silica gel chromatography was conducted with Fisher Scientific 60 (100-200 mesh) silica gel, and alumina adsorption chromatography was conducted with Fisher Scientific non-treated (80-200 mesh) alumina adsorption. Reagents and solvents were of commercial grade and used as supplied with the following exceptions: Ethanol was distilled from magnesium metal. Di-2-pyridyl ketone was recrystallized from diethyl ether. Reactions were carried out in flame-dried or oven-dried glassware under an atmosphere of nitrogen.

Synthesis of Sodium *O*-ethylmethylphosphonodithioate (4)

The white solid 4 (915 mg, 30%) was prepared according to a literature method²³: ^1H NMR (acetone- d_6) δ 3.92 (dq, $J = 7.5, 9.0$ Hz, 2H), 1.83 (d, $J = 15.0$

Hz, 3H), 1.15 (t, $J = 7.5$ Hz, 3H); ^{13}C NMR (acetone- d_6) δ 57.6 (d, $J = 30$ Hz), 32.8 (d, $J = 330$ Hz), 15.9 (d, $J = 30$ Hz).

Synthesis of Ethyl 5-amino-6,6-(2,2'-dipyridyl)hexanoate (5)²⁴

To a stirred solution of ethyl 4-aminobutyrate hydrochloride (1.4 g, 8.4 mmol) in methanol (5 mL) was added sodium cyanoborohydride (112 mg, 1.79 mmol) and di-2-pyridyl ketone (328 mg, 1.78 mmol), and the resulting mixture was heated at reflux for 23 h. The reaction mixture was cooled to room temperature and filtered; the solvent was removed from the filtrate *in vacuo*. The resulting oil was dissolved in water (10 mL), acidified to pH = 2, and extracted with diethyl ether (3 x 10 mL). The pH of the aqueous layer was raised to 10, and it was extracted with diethyl ether (3 x 10 mL). The combined basic extracts were concentrated *in vacuo*, and the residue was subjected to column chromatography (silica gel, methanol followed by alumina adsorption, 10% methanol in dichloromethane) to give **5** (152 mg, 29%) as a colorless, luminescent oil: ^1H NMR (CD_3OD) δ 8.49 (d, $J = 8.1$ Hz, 2H), 7.76 (t, $J = 8.1$ Hz, 2H), 7.50 (d, $J = 7.5$ Hz, 2H), 7.25 (t, $J = 6.0$ Hz, 2H), 5.19 (s, 1H), 4.06 (q, $J = 7.5$ Hz, 2H), 2.57 (t, $J = 7.0$ Hz, 2H), 2.36 (t, $J = 7.2$ Hz, 2H), 1.84 (qn, $J = 7.8$ Hz, 2H), 1.19 (t, $J = 6.6$ Hz, 3H); ^{13}C NMR (CD_3OD) δ 173.7, 160.7, 148.5, 137.1, 122.5, 122.4, 68.7, 60.0, 46.5, 31.5, 24.7, 13.1.

Synthesis of [5-Amino-6,6-(2,2'-dipyridyl)hexanoic acid]-dichloroplatinum (II) (6)

To a stirred solution of **5** (100 mg, .334 mmol) in water (8 mL) was added 12 M HCl (5 drops) followed by potassium tetrachloroplatinate (II) (130 mg, .312 mmol). The resulting solution was heated at reflux for 7 h. The reaction mixture was cooled

to room temperature and filtered. The yellow precipitate **6** (101 mg, 56%) was washed extensively with water and dried in a vacuum oven: ^1H NMR (DMSO- d_6) δ 9.00 (d, J = 6.0 Hz, 2H), 8.14 (t, J = 7.5 Hz, 2H), 7.95 (d, J = 8.1 Hz, 2H), 7.54 (t, J = 6.3 Hz, 2H), 6.35 (s, 1H), 3.65 (t, J = 6.6 Hz, 2H), 2.27 (t, J = 7.8 Hz, 2H), 2.03 (p, J = 6.9 Hz, 2H); ^{13}C NMR (DMSO- d_6) δ 153.9, 152.6, 140.4, 128.8, 126.4, 65.0, 61.5, 47.4, 30.9, 18.9. Anal. Calcd for $\text{C}_{15}\text{H}_{17}\text{Cl}_2\text{N}_3\text{O}_2\text{Pt}$: C, 33.53; H, 3.19; N, 7.82. Found: C, 33.81; H, 2.85; N, 7.86.

Conclusions

Although the goal of synthesizing a transition state analogue for $\{(2,2'\text{-dipyridylamine})\text{Cu}(\text{OH})_2\}^{2+}$ catalyzed hydrolysis of ethyl acetate was not realized, some interesting information was obtained through this study. A method for functionalizing di-2-pyridyl ketone was accomplished. The method is unattractive because of the complicated chromatography series required to purify the product, but it illustrates a significant point, i.e. reductive amination using a di-aryl ketone is possible. The relative strength of the interaction between platinum and sulfur was examined. The magnitude of the relative strength of the platinum-sulfur interaction over the platinum-nitrogen interaction was unforeseen. The observation that the phosphonodithioate ligand displaces the dipyridylamine ligand on platinum implies that the metal-sulfur interaction is much stronger than the metal-nitrogen interaction.

Development of a metalloabzyme by incorporation of a metal complex cofactor into the transition state stabilization approach is a valid strategy and needs to be investigated further. There are possible ways to improve the procedure discussed in

this chapter so that an appropriate hapten could be synthesized. A more practical way to functionalize the dipyridyl ligand should be employed. The loss of product in the chromatography steps makes it difficult to isolate conjugatable ligand. It would be beneficial to have a species that is more stable and thus easier to store, as well. The phosphonodithioate ligand should be replaced with a species that contains one oxygen and one sulfur donor atom rather than two sulfur donor atoms so that there is less chance of displacement of the dipyridyl ligand. A thiophosphonic acid monoester would fulfill this requirement. These esters have been synthesized using thiophosphonic acid ester halides and diluted base²⁶ as well as phosphonic acid ester halides and sodium hydrogen sulfide.²⁷

CHAPTER 3

SEMI-SYNTHETIC PROCEDURE: PREPARATION OF A METALLOANTIBODY

Introduction

In order to incorporate a metal complex cofactor into the semi-synthetic procedure for abzyme production, a metal complex must be introduced into the binding site of an antibody of known specificity. During this research, Nakayama and Schultz reported attempts to develop semi-synthetic catalytic antibodies that are metal dependent.²⁸ Using the method described by Pollack and coworkers (Figure 3.1),¹¹ the binding site of the MOPC-315 antibody Fab fragment was chemically modified with cyclam (1,4,8,11-tetraazacyclotetradecane) and 1,10-phenanthroline in order to introduce a specific metal binding site into the antibody. These ligands were chosen because they have been used successfully in a number of enzyme model studies.²⁹ It was anticipated that the altered Fab fragment would bind a metal ion at the modified site and the resulting semi-synthetic antibody would catalyze oxidation or hydrolysis reactions, depending on the metal ion used. The cyclam derivitized Fab was found to catalyze hydrolysis of a coumarin ester substrate in the absence of metal ion. However, in the presence of the metal ions cobalt(II), copper(II), gallium(III), iron(II), nickel(II), zinc(II), these semi-synthetic antibodies did not catalyze the desired reactions.

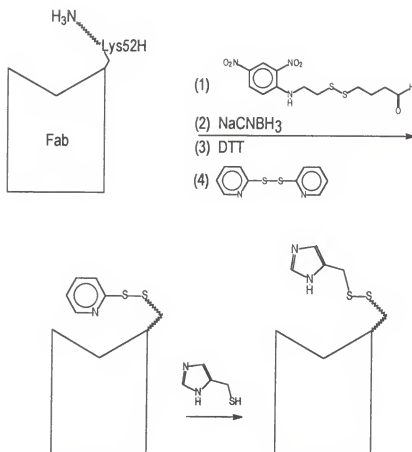


Figure 3.1
Preparation of a semi-synthetic abzyme

There are several possible reasons for the lack of metal ion-dependent catalytic activity by the semi-synthetic antibodies, as explained by Nakayama and Schultz.²⁸

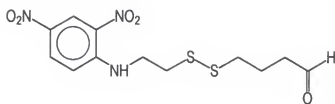
One reason is that the cyclam and the 1,10-phenanthroline attached to the Fab may not complex metal ions efficiently under the conditions used. In support of this proposal, electron paramagnetic resonance studies for one case showed that the copper(II) ion was bound non-specifically by the derivitized Fab, but it was not bound by the chelator ligand; the reason for the lack in binding is not apparent. The problem may result from ligation of the cyclam and 1,10-phenanthroline metal ion complexes by residues on the surface of the Fab binding site, a situation that would prevent the complex from interacting with substrate. It is also possible that metal complex orientation prohibits productive interactions with bound substrate. Further study is necessary to determine if a MOPC-315 antibody linked with a metal complex can cause rate acceleration.

The goal of this work was to develop a semi-synthetic metalloabzyme by modifying the MOPC-315 binding site with the $\{(2,2'\text{-dipyridylamine})\text{Cu}(\text{OH}_2)_2\}^{2+}$ complex (**1**). As **1** has been shown to be an efficient catalyst for the hydrolysis of esters and amides,¹⁶ it was anticipated that an antibody modified with it could be used to study the plausibility of a semi-synthetic metalloantibody hydrolysis catalyst. The preparation of a $\{(2,2'\text{-dipyridylamine})\text{Cu}(\text{OH}_2)_2\}^{2+}$ modified MOPC-315 Fab will be discussed in this chapter.

Synthetic Plan

Preparation of the metalloantibody was accomplished in four steps. The first step was isolation of MOPC-315 Fab fragment. MOPC-315 Fab was chosen because of its binding specificity for nitrophenyl groups. The semi-synthetic approach used was based on Schultz's work in which MOPC-315 served as a suitable antibody for catalysis of dinitrophenyl esters.¹¹ MOPC-315 is a well studied antibody of the IgA class, and methods for its purification and fragmentation are readily available.¹²

The second step in metalloantibody preparation was synthesis of the substance which was to link the MOPC-315 antibody to the catalyst (the substance is known informally as the linker). Linker preparation was outlined in Schultz's work¹¹, and the requirements placed on the linker are as follows. The substance must be capable of reversible binding to MOPC-315. This capability allows the linker to be placed in the necessary position for covalent attachment near the antibody binding site. The substance must contain a functional group that will allow it to react with a group on the antibody and thus facilitate covalent attachment. Finally, the substance must be cleavable in such a way that, upon cleavage, a reactive species that can undergo condensation with the catalyst is left; this provides a means for attaching the catalyst in close proximity to the binding site of the antibody. The compound (*N*-2,4-dinitrophenyl)-2-aminoethyl 4-oxobutyl disulfide (**11**) (Figure 3.2) fulfills all of the requirements. The dinitrophenyl group allows for non-covalent binding by MOPC-315, and the aldehyde allows for a covalent linkage between the two entities. The disulfide linkage provides a means for cleaving the covalently connected linker such



11

Figure 3.2
(*N*-2,4-Dinitrophenyl)-2-aminoethyl 4-oxobutyl disulfide,
Linker

that a reactive thiol is left. Schultz found that this compound's length was optimal for binding of the dinitrophenyl moiety in the MOPC-315 binding site with simultaneous reaction of the aldehyde portion with an amino acid of the antibody, Lys52H.

The next stage in metalloantibody preparation was synthesis and functionalization of the metal complex catalyst. First, the dipyridylamine ligand was functionalized; it was necessary to attach a functional group to the amine nitrogen to provide a means for the ligand (and the complex) to be joined to the antibody. The conditions under which 2,2'-dipyridylamine will react were determined,³⁰ and a four carbon chain with a thiol functionality was attached to the amine nitrogen. This functionalized ligand was used to make a copper complex. The complex [4-(2,2'-dipyridylamine)butanethiol]copper(II) chloride was chosen as a precursor to the diaqua complex so that the catalyst could be characterized as a solid. The diaqua complex is formed upon dissolution of [4-(2,2'-dipyridylamine)butanethiol]copper(II) chloride in water.

The final stage in this preparation involved combining of the three separate species - antibody, linker, and functionalized catalyst - to make a metalloantibody. The procedure for doing this was outlined in Schultz's work.¹¹ The antibody and the linker were combined, and the linker was non-covalently bound by the antibody via the dinitrophenyl group. The aldehyde functionality on the linker was in the correct position to react with an amine functionality on Lys52H in reductive amination; the result of this reaction was a covalent connection between antibody and linker. The dinitrophenyl portion of the linker was cleaved off and washed away to afford thiol-

labeled antibody. The thiol-labeled antibody was then allowed to react with thiol-labeled dipyridylamine. The resulting dipyridylamine-modified Fab was incubated with copper (II) chloride ion to give the working metalloantibody. Figure 3.3 shows the overall synthetic plan.

Results and Discussion

Isolation of MOPC-315 Fab Fragment

A procedure described by Goetzl and Metzger was used to purify the MOPC-315 antibody.^{12b} The major step in the purification was affinity chromatography using dinitrophenyl-labeled sepharose; this step served to separate the dinitrophenyl-binding protein, MOPC-315, from all other proteins present in the ascites sample.

The MOPC-315 IgA was digested according to a procedure illustrated by Eisen, Simms, and Potter.^{12a} This procedure involved cleavage using papain, a thiol protease derived from papaya. Papain cleaves antibody molecules in the hinge region to yield two Fab fragments and an Fc fragment. The Fc fragment is broken down further by secondary action of the enzyme, but the Fab fragments remain intact.³¹ The Fab fragments were isolated from other fragments using dialysis.

Characterization of MOPC-315 Fab was at first confusing. The results of 4 to 10% gradient SDS polyacrylamide-gel electrophoresis implied an Fab molecular mass of 25,000 to 30,000, numbers that are lower than the expected value of around 50,000 (Figure 3.4). However, covalent disulfide bridges that are usually found between the immunoglobulin heavy and light chains of antibody molecules are absent in IgA

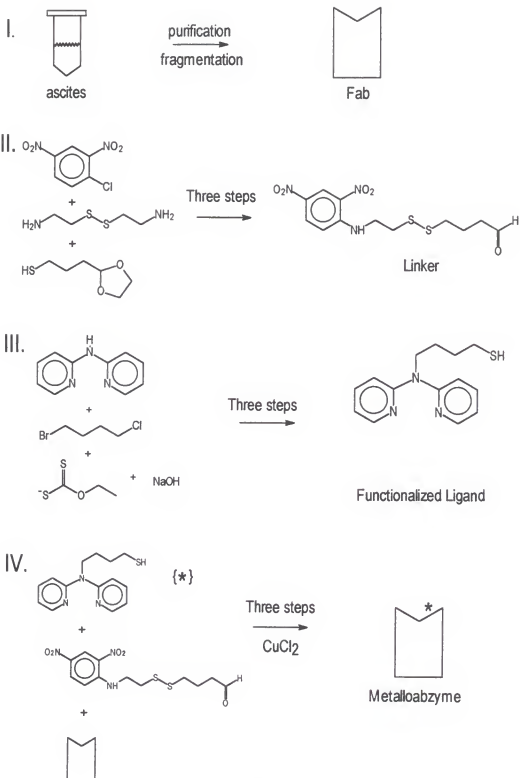


Figure 3.3
Scheme for preparation of a metalloantibody

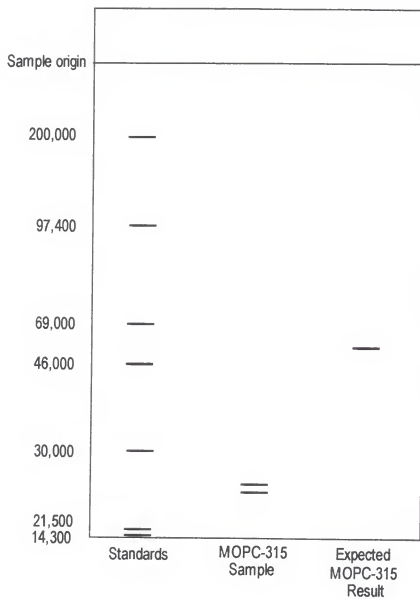


Figure 3.4
MOPC-315 Fab 4-10% SDS-PAGE gel electrophoresis results

obtained from BALB/c mice.³² This results in dissociation of light and heavy chains in the presence of sodium dodecyl sulfate sample buffer which in turn leads to gel bands at lower molecular masses than bands for the intact Fab. The molecular mass of the Fab fragment was determined to be 55,000 with gel filtration FPLC, a technique that does not disrupt the non-covalent interactions holding the heavy and light chains together. Figure 3.5 shows the FPLC elution peak for MOPC-315 Fab. The molecular mass was obtained from a calibration curve of standards.

The affinity of the antibodies for the dinitrophenyl group was characterized using enzyme linked immunoabsorbent assay (ELISA). The ELISA plates were coated with dinitrophenyl-labeled bovine serum albumin. Of several different blocking buffers investigated (5% non-fat dry milk, 10% horse serum, gelatin, bovine serum albumin), 0.1 M glycine gave the best results. The secondary antibody used was an α chain specific anti-IgA antibody elicited in goat. This antibody was linked to the enzyme alkaline phosphatase, and *p*-nitrophenyl phosphate was used as the substrate. Typically, a μ g concentration of Fab gave A_{405} readings of 0.550 after 1 minute in substrate. All antibody samples were stored at 4°C.

Synthesis of the Linker

Synthesis of **11** proved to be difficult because many of the traditional methods used for making thiols from halides³³ would not work for 2-(3-chloropropyl)-1,3-dioxolane (**13**), one of the necessary halide starting materials. The method that finally proved effective, reaction of the dioxolane with sodium trithiocarbonate,³⁴ was successful possibly because of the driving force associated with evolution of the gas



Figure 3.5
Elution peak of MOPC-315 Sephacryl S-100-HR FPLC

carbon disulfide. The other steps in the synthesis were straightforward, as described by Pollack et al. (Figure 3.6).¹¹

Functionalization of the Metal Complex Ligand, 2,2'-Dipyridylamine

Functionalization of the 2,2'-dipyridylamine ligand (**16**) was carried out in a series of steps (Figure 3.7). In order to make the amine nitrogen more nucleophilic, and thus more reactive, **16** was allowed to react with potassium hydroxide in dimethyl sulfoxide. The strong base removed the proton from the amine nitrogen making the nitrogen a stronger nucleophile. The choice of which reaction solvent and which base to use is critical. The experiment was attempted using several different combinations: potassium hydroxide in dimethyl sulfoxide, sodium hydroxide in dimethyl sulfoxide, potassium hydroxide in dimethyl formamide, sodium hydroxide in dimethyl formamide. The best combination is potassium hydroxide in dimethyl sulfoxide; changing only one of these species decreases the yield of product by approximately 30%, and changing both decreases the yield by more than 50%.

The deprotonated amine was allowed to react with a dihalide, 1-bromo-4-chlorobutane (**18**). In general, bromides are better leaving groups than chlorides in substitution reactions such as this one because the bromide-carbon bond is weaker and thus more easily broken than the chloride-carbon bond. Consequently, the bromide functionality reacted with **18** preferentially to give (N-4-chlorobutyl)dipyridylamine (**19**).

It was necessary to introduce a thiol group into the catalyst so that it could be connected to the antibody through a disulfide bond. With this in mind, **19** was allowed

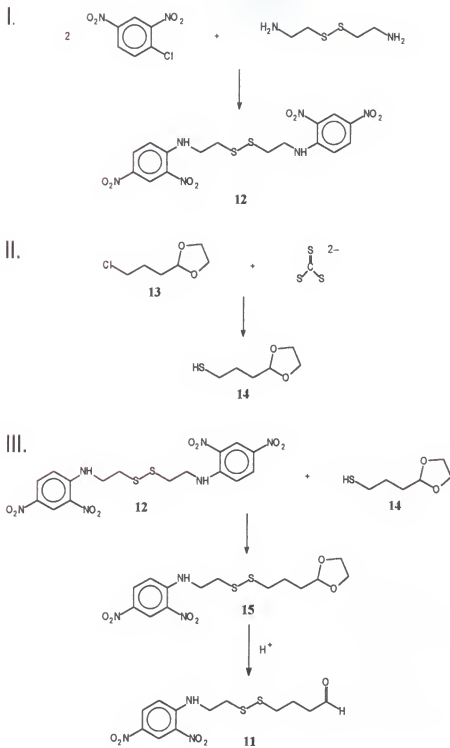


Figure 3.6
Outline for synthesis of the linker

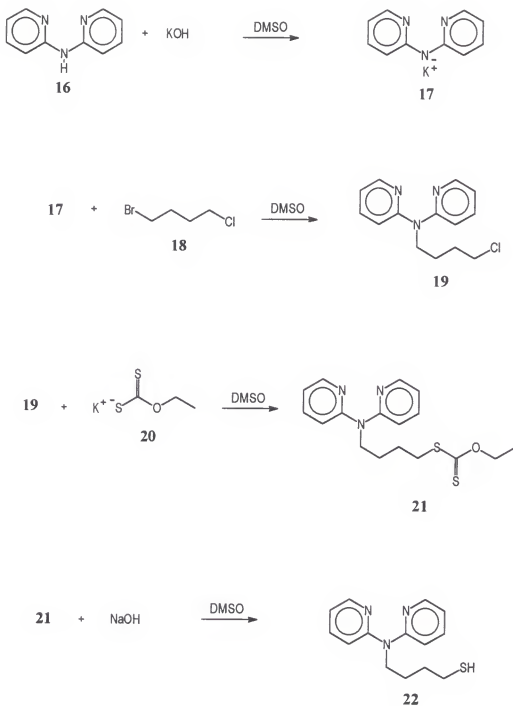


Figure 3.7
Functionalization of 2,2'-dipyridylamine

to react with the potassium salt of *O*-ethylxanthic acid (**20**) in order to make *S*-(*N,N*-dipyridyl)-4-aminobutyl *O*-ethylxanthate (**21**), the precursor to thiol. Again, the reaction solvent affects the yield; dimethyl sulfoxide gave the best results for this particular starting material. The xanthate was cleaved using 10% sodium hydroxide to give thiol (**22**). All substances were stored in the dark at 4°C to avoid decomposition.

Preparation of the Metalloantibody

The MOPC-315 Fab was activated for attachment of catalyst according to the method established by Schultz and coworkers.¹¹ The Fab was combined with **11** so that the dinitrophenyl group would attach non-covalently to the binding site of the antibody fragment. The Fab-linker complex was then allowed to react with an excess of sodium cyanoborohydride to induce reductive amination between the aldehyde functionality on the linker and the amine functionality on the Fab (Lys52H). Gel filtration chromatography was used to separate the relatively large Fab-linker complex from the relatively small sodium cyanoborohydride molecules. The sample was then run over a dinitrophenyl-labeled Sepharose column. This step served to separate the linker-labeled Fab from any non-labeled Fab. The non-labeled Fab has an accessible binding site and will bind to dinitrophenyl groups attached to the column, whereas the labeled Fab has no free binding site and will flow through the column.

The disulfide bond of the linker was cleaved using dithiothreitol to give a free thiol functionality on the Fab. The *N,N'*-bis(2,4-dinitrophenyl)cystamine that resulted was removed using gel filtration chromatography. Eluted Fab was allowed to flow directly into a solution of aldrithiol so that the free thiol on the fragment would react

to produce pyridine-labeled Fab. This served to put a good leaving group on the Fab; when the disulfide bond between antibody fragment and pyridine is broken, thiopyridone results. At this point, the derivatized Fab was ready to accept catalyst.

The 2,2'-dipyridylamine ligand was attached to MOPC-315 in the same way that Pollack et al. attached imidazole to this antibody.^{11b} The method proved be very straightforward. The thiopyridyl disulfide adduct of the antibody was incubated with **22**, and the thiol functionality on dipyridylamine reacted with the disulfide functionality on the antibody. The reaction was easily followed by monitoring the release of the thiopyridone product, which absorbs at 343 nm. Quantitative release of thiopyridone was observed.

The metalloantibody was generated by exposing dipyridylamine-functionalized Fab to an excess of copper(II) ion. A ten-fold excess was used to ensure binding of copper by the dipyridylamine group in addition to non-specific binding by amino acid residues. Presumably, the excess pushed the equilibrium toward complex formation with dipyridylamine. The overall scheme for preparation of the metalloantibody is shown in Figure 3.8.

Experimental Methods

General Procedures

Proton NMR and ¹³C NMR spectra were recorded at 300 MHz on a General Electric QE-300 spectrometer or a Varian Gemini-300 spectrometer. Chemical shifts are reported in parts per million; the residual solvent peak was used as an internal

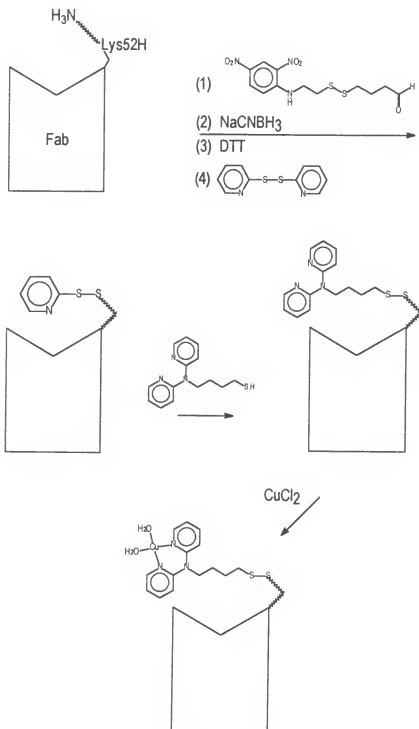


Figure 3.8
Semi-synthetic metalloantibody preparation

standard. Elemental analysis (C,H,N) was performed by the University of Florida Department of Chemistry Analytical Services. The plasmacytoma MOPC-315 was obtained from the American *Type Culture* Collection. Amicon Centriprep 10 and Centriplus 10 were used for filtration centrifugation. Reagents and solvents were of commercial grade and used as supplied. Aldrithiol-2, or 2,2'-dipyridyl disulfide, was obtained from Aldrich.

Maintenance of Tumor

The MOPC-315 IgA secreting myeloma cells were maintained and harvested by the Hybridoma Core Laboratory, Interdisciplinary Center for Biotechnology Research, University of Florida, P.O. Box 100275, Gainesville, FL 32611. The plasmacytoma MOPC-315 was propagated in Balb/c mice by injecting a tumor suspension into the abdomen. This tumor suspension was injected intraperitoneally into pristane-primed mice to produce ascites. By an average of 14 days a significant amount of ascites had formed, and each mouse was tapped three times to collect the antibody-containing fluid. Typically, a total yield of 5 mL ascites per surviving mouse was obtained. Ascites was stored frozen prior to purification.

Purification of MOPC-315

The MOPC-315 antibody was purified according to a procedure outlined by Goetzl and Metzger.^{12b} Ascites was extracted with 1,1,2-trichlorotrifluoroethane, filtered, and dialyzed against 0.2 M Tris-HCl buffer (pH 8.6) at 4°C overnight. The clarified ascites sample was reduced in 0.1 M dithiothreitol for 1 h at 25°C, diluted 1:1 with 0.2 M Tris-HCl buffer (pH 7.3), and alkylated in 0.11 M iodoacetamide for 15

minutes at 25°C. The solution was then dialyzed against 0.015 M sodium borate, 0.15 M sodium chloride buffer (pH 8.0) at 4°C overnight. The reduced and alkylated ascites was applied to an ϵ -N-DNP-lysine-Sepharose column³⁵ (12 cm x 2.5 cm). Prior to each run, the column was put through a washing protocol. One percent bovine serum albumin (30 mL) was applied to the column and washed through with borate-saline buffer (~ 250 mL). Twenty-five percent acetic acid (40 mL) was then applied and washed through with the borate-saline buffer (~ 700 mL). In a typical run, 35 mL ascites was diluted to 90 mL with borate-saline buffer, and the diluted ascites was applied to the washed column. In addition to application of the original sample, the eluate was reapplied three times. The column was washed with 250 mL borate-saline buffer. MOPC-315 was then specifically eluted by adding 0.1 M DNP-glycine (pH ~ 9.0, 10 mL). The orange-yellow eluate was collected and concentrated by filtration centrifugation to 7.5 mL. The bound DNP-glycine was removed by passing the sample over a Dowex 1-X8 (20 - 50 mesh) column (6.5 cm x 2.5 cm) using 0.01 M sodium phosphate, 0.1 M sodium chloride buffer (pH 5.7). The average yield was ~ 0.3 mg protein per mL ascites. The concentration of MOPC-315 antibody was determined by ultraviolet absorbance where $\epsilon_{280\text{nm}}$ for a 0.1% solution is equal to 1.44.

Isolation of Fab Fragment

The procedure used for isolation of Fab fragment was based on one described by Eisen, Simms, and Potter.^{12a} Papain (10 mg) was added to a solution of dithiothreitol (0.2 μg , .001 μmol) in 0.055 M phosphate, 0.004 M EDTA buffer (pH 7.3), and the sample was incubated at 37°C for 10 minutes. The reaction mixture was

run over a Sepadex G25 column (d 10 mm, l 60 mm) using the phosphate-EDTA buffer to elute papain. The absorbance was monitored at 280 nm, and papain concentration was calculated using $E_{1\text{ cm}, 280}^{1\%} = 25$. MOPC-315 (18 mg, 0.15 μmol) was incubated with activated papain (265 μg , 1.5% the weight of the protein) for 30 minutes at 37°C, and the sample was dialyzed against 0.1 M phosphate, 0.15 M sodium chloride buffer (pH 7.3). The sample was run over a Sephacryl S-100-HR column using FPLC, and MOPC-315 Fab (7.8 mg, 47%) was eluted as a 1.5 mg/mL solution in phosphate buffered saline.

Synthesis of 2-*N*-(2,4-dinitrophenyl)-aminoethyl 4-oxobutyl disulfide (11)¹¹

The orange-yellow solid **11** (32 mg, 10%) was prepared according to the Pollack et al. method^{11b}: ¹H NMR (CDCl₃) δ 9.16 (d, *J* = 2.6 Hz, 1H), 8.79 (s, 1H), 8.32 (dd, *J* = 9.5, 5.0 Hz, 1H), 7.01 (d, *J* = 9.5 Hz, 1H), 4.87 (t, *J* = 4.2 Hz, 1H), 3.90 (m, 6H), 2.99 (t, *J* = 6.7 Hz, 2H), 2.78 (t, *J* = 7.0 Hz, 2H), 1.87 (m, 4H).

Functionalization of 2,2'-Dipyridylamine

Synthesis of (*N*-4-chlorobutyl)dipyridylamine (19)³⁰

To a stirred solution of 2,2'-dipyridylamine (1.71 g, 10.0 mmol) in dimethyl sulfoxide (15 mL) was added potassium hydroxide (2.6 g, 46.3 mmol). The reaction mixture was stirred at 25°C for 6 h, and 1-bromo-4-chlorobutane (1.40 mL, 12.1 mmol) was added. After being stirred at 25°C for an additional 11 h, the mixture was dissolved water (30 mL) and extracted with dichloromethane (3 x 50 mL). The organic layer was washed with water (50 mL) and dried over magnesium sulfate. The mixture was filtered, and solvent was removed from the filtrate *in vacuo* to give **19**

(1.39 g, 53%) as a crimson liquid: ^1H NMR (CDCl_3) δ 8.27 (d, J = 6.2 Hz, 2H), 7.48 (t, J = 7.7 Hz, 2H), 7.04 (d, J = 8.5 Hz, 2H), 6.84 (t, J = 5.8 Hz, 2H), 4.20 (t, J = 7.7 Hz, 2H), 3.55 (t, J = 6.9 Hz, 2H), 1.80 (q, J = 5.0 Hz, 4H); ^{13}C NMR (CDCl_3) δ 157.1, 148.2, 137.0, 116.9, 114.5, 47.0, 44.8, 29.9, 25.6.

Synthesis of *S*-(*N,N*-dipyridyl)-4-aminobutyl *O*-ethylxanthate (**21**)^{33c,d,e}

To a solution of **19** (1.01 g, 3.86 mmol) in dimethyl sulfoxide (10 mL) was added **20** (1.00 g, 6.24 mmol). The reaction mixture was stirred at 25°C for 72 h and then dissolved in water (30 mL). The pH of the solution was adjusted to neutral, and it was extracted with dichloromethane (3 x 50 mL). The organic layer was washed with water (50 mL) and dried over magnesium sulfate. The mixture was filtered, and solvent was removed from the filtrate *in vacuo* to give **9** (1.11 g, 83%) as a brown liquid: ^1H NMR (CDCl_3) δ 8.34 (d, J = 4.8 Hz, 2H), 7.48 (t, J = 7.6 Hz, 2H), 7.06 (d, J = 8.4 Hz, 2H), 6.82 (t, J = 6.0 Hz, 2H), 4.63 (J = 6.3 Hz, 2H), 4.20 (t, J = 6.5 Hz, 2H), 3.13 (J = 6.5 Hz, 2H), 1.70 (m, 4H), 1.40 (t, J = 6.8 Hz, 3H); ^{13}C NMR (CDCl_3) δ 157.3, 148.3, 137.0, 116.8, 114.7, 114.5, 47.3, 41.0, 31.3, 26.9, 24.3, 13.7.

Synthesis of *N,N*-dipyridyl-4-amino-1-butanethiol (**22**)^{33c,d,e}

To a solution of **21** (278 mg, 0.800 mmol) in methanol (10 mL) was added sodium hydroxide (1.5 g, 37.5 mmol) in water (7.5 mL), and the reaction mixture was stirred at 25°C for 2 h. The pH of the reaction mixture was lowered to 2, and it was extracted with dichloromethane (3 x 50 mL). The organic layer was washed with water (50 mL) and dried over magnesium sulfate. The mixture was filtered, and solvent was removed from the filtrate *in vacuo* to give **22** (55 mg, 27%) as a yellow

oil: ^1H NMR (CDCl_3) δ 8.26 (d, $J = 7.6$ Hz, 2H), 7.44 (t, $J = 9.1$ Hz, 2H), 7.02 (d, $J = 8.3$ Hz, 2H), 6.80 (t, $J = 7.3$ Hz, 2H), 4.17 (t, $J = 8.1$ Hz, 2H), 2.50 (m, 2H), 1.70 (m, 4H), 1.36 (t, $J = 7.4$ Hz, 1H); ^{13}C NMR (CDCl_3) δ 157.1, 148.1, 137.0, 116.8, 114.5, 47.2, 31.2, 26.8, 24.2.

Derivatization of Fab for Dipyrldylamine Attachment¹¹

To MOPC-315 Fab (3.9 mg, 0.071 μmol) in 0.1 M phosphate, 0.15 M sodium chloride buffer (pH 7.3) was added **11** (36.7 μg , 0.11 μmol). The reaction solution was incubated at 37°C for 1 h. Sodium cyanoborohydride (33.4 μg , 0.53 μmol) was added, and the solution was incubated at 37°C for an additional 20 h. The sample was run over a Sephadex G50 column (d 1.6 cm, l 6.5 cm) using phosphate buffered saline to elute. The fractions that contained protein, as indicated by A_{280} , were pooled and concentrated by filtration centrifugation. The concentrated sample was run over a dinitrophenyl-labeled Sepharose column (d 1.6 cm, l 6.0 cm); the linker-labeled MOPC-315 Fab (1.6 mg, 0.029 μmol) was eluted in 0.015 M sodium borate, 0.15 M sodium chloride buffer (pH 8.0).

To the linker-labeled Fab (1.6 mg, 0.029 μmol) in phosphate buffered saline was added 0.1 M phosphate, 100 mM dithiothreitol, 4 mM EDTA (pH 8.0, 1 mL). The reaction solution was incubated at 37°C for 12 h and then applied to a Sephadex G25 column (d 1.6 cm, l 6.0 cm). Using phosphate buffered saline as the solvent, the Fab was eluted directly into a 0.1 M phosphate, 4.5 mM aldrithiol-2, 15% acetonitrile solution (pH 5.8, 1 mL). The sample was allowed to incubate at 25°C for 28 h. The

free thione was dialyzed away by filtration centrifugation to leave pyridine-labeled Fab (0.67 mg, 0.012 μmol) in phosphate buffered saline.

Attachment of Dipyrldylamine to Fab Fragment¹¹

To pyridine-labeled MOPC-315 Fab (1.1 mg, 0.02 μmol) in 0.1 M sodium phosphate, 0.15 M sodium chloride (pH 7.3, 2.5 mL) was added **22** (51.8 mg, 0.2 μmol). The reaction mixture was incubated at 20°C for 45 min. Dipyrldylamine incorporation was followed by monitoring the release of 2-thiopyridone spectrophotometrically; 2-thiopyridone absorbs at 343 nm with an ϵ of 7060 $\text{M}^{-1} \text{cm}^{-1}$.³⁶ Thiopyridone and excess *N,N*-dipyrldyl-4-amino-1-butanethiol were removed via filtration centrifugation. The dipyrldylamine-labeled antibody fragment (0.94 mg, 85%) was retained in the phosphate buffered saline.

Preparation of the Metalloantibody

To dipyrldylamine-labeled MOPC-315 Fab (0.47 mg, 0.0085 μmol) in 0.1 M phosphate buffer (pH 7.0, 1.0 mL) was added copper(II) chloride (11.4 mg, 0.085 μmol). The reaction mixture was incubated at 25°C for 3 minutes before use in kinetic studies.

Conclusions

Preparation of the metalloantibody turned out to be more complicated than was originally anticipated. This was due mainly to the problems that arose in synthesis of the linker and characterization of the MOPC-315 Fab fragment that were mentioned earlier. Other minor difficulties were encountered, as well. The intermediate

compounds synthesized in preparation of functionalization of the 2,2'-dipyridylamine, i.e. (*N*-4-chlorobutyl)dipyridylamine and *S*-(*N,N*-dipyridyl)-4-aminobutyl *O*-ethylxanthate, proved to be very unstable and could not be stored for very long. This made it very difficult to obtain pure functionalized dipyridylamine which was necessary to ensure homogeneous modified antibody. Another complication was the relatively large loss of protein during concentration and dialysis. Most of the methods for concentration and dialysis of proteins are accompanied by a loss of one or more milligrams of sample. Considering that the ascites gave a relatively low yield of MOPC-315 antibody to begin with (0.3 mg of protein per mL ascites) and that there are several chromatography steps where loss could occur in the Fab isolation procedure, any additional loss in sample was devastating.

In spite of the obstacles encountered, an antibody functionalized with 2,2'-dipyridylamine was generated. Presumably, the dipyridylamine will bind copper (II) ion in solution to give a metal catalyst-functionalized form of the antibody. The antibody will bind esters that contain dinitrophenyl groups due to its binding site specificity. The metal complex catalyst that is in such close proximity to the bound substrate should then induce rate enhancement of ester hydrolysis.

CHAPTER 4

PRELIMINARY KINETIC STUDIES ON METALLOANTIBODY CATALYZED HYDROLYSIS OF ESTERS

Introduction

The first stage in assessment of the $\{(2,2'\text{-dipyridylamine})\text{Cu}(\text{OH}_2)_2\}^{2+}$ complex-modified antibody as a hydrolysis catalyst was to determine if the antibody could cause rate acceleration for a representative reaction. This required establishment of appropriate kinetic methods. There are many factors that may affect the rate constant of a chemical reaction. Temperature, pH, ionic strength, and solution species concentrations are conditions that must be considered. The method for following the reaction rate must be chosen so that the aforementioned conditions may be optimized. All of these considerations taken together give rise to an appropriate kinetic system.

The original reaction chosen for study was hydrolysis of 2,4-dinitrobenzoic acid, 7-hydroxycoumarin ester (**23**) (Figure 4.1). This ester was used successfully in studies of imidazole-functionalized MOPC-315 Fab to demonstrate that abzyme's catalytic ability.^{11c} However, investigation of the hydrolysis reaction using **1** as a catalyst indicated that it would be inappropriate for study with the metalloantibody. The hydrolysis of 2,4-dinitrophenyl acetate (**24**) (Figure 4.2) was then considered. This compound is similar to the ester *p*-nitrophenyl acetate, a substance that has

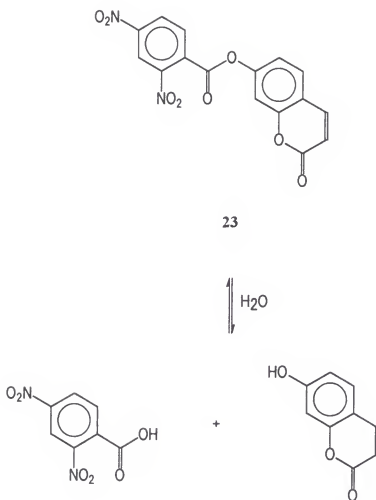


Figure 4.1
Hydrolysis of 2,4-dinitrobenzoic acid, 7-hydroxycoumarin ester

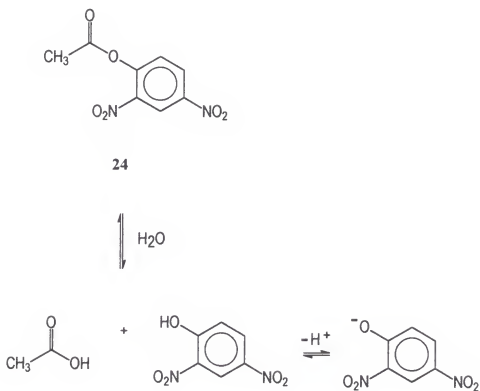


Figure 4.2
Hydrolysis of 2,4-dinitrophenyl acetate

proven to be a suitable substrate for studies with the copper complex catalyst.¹⁶

Kinetic studies designed to demonstrate the capability of {(2,2'-dipyridylamine)Cu(OH)₂}²⁺-modified MOPC-315 Fab to act as a hydrolysis catalyst are described herein.

Results and Discussion

Copper Complex Catalyzed Reactions

Before examining the catalytic ability of the metalloabzyme, it was necessary to characterize the catalytic behavior of **1**. Initially, the compound 2,4-dinitrobenzoic acid, 7-hydroxycoumarin ester was chosen as a substrate because it has been used successfully as an ester hydrolysis substrate in numerous other abzyme studies.¹¹ The dinitrophenyl group allows for binding by the MOPC-315 antibodies. Thus, the substrate is capable of being drawn into close proximity to the catalyst near the binding site. The coumarin functionality is important in following the reaction rate. Upon hydrolysis, the ester will release 7-hydroxycoumarin. When excited at 355 nm, the alcohol emits at 461 nm, and its release can be quantitated fluorometrically. Figure 4.1 shows the hydrolysis of **23**.

The conditions for collection of rate data were chosen such that catalyst activity would be favorable. The active water molecule on the copper complex has a pK_a of 7.2.¹⁶ Since the active form of the catalyst contains a hydroxide group (the active water molecule is deprotonated), the pH could be no lower than approximately 6.6. Also, the system was designed to be consistent with typical physiological

conditions, and a pH of 7.0 was maintained using 0.1 M phosphate buffer. The reaction temperature was chosen to be 25°C. The concentration of 2,4-dinitrobenzoic acid, 7-hydroxycoumarin ester was selected to be 1 μ M, a value that falls nicely into the detection range of the SPEX fluorimeter.

Preliminary studies involving hydrolysis of **23** in the presence of 1 mM **1** showed no rate enhancement over background; the copper complex had no effect at all on initial reaction rate (Figure 4.3). It is possible that the copper complex cannot bind the ester appropriately due to the steric bulk of the dinitrobenzyl and coumarin groups. Most of the substrates Chin and coworkers have studied with the copper complex have been relatively small with unhindered carbonyl carbons, e.g. methyl acetate, formamide, and *N,N*-dimethylformamide.¹⁶ The proposed mechanism of copper complex catalyzed hydrolysis requires that the copper-coordinated hydroxide attack the carbonyl carbon of the substrate, and this may not be favored for **23**. Because the catalytic ability of the metalloantibody is theoretically dependent on the activity of the basic copper complex as a catalyst, the lack of activity observed required that a different substrate be investigated.

The next step in development of an appropriate kinetic system was to confirm the activity of the copper complex under the desired reaction conditions. Chin et al.¹⁶ have reported a rate constant of $1.6 \times 10^{-1} \text{ M}^{-1} \text{ s}^{-1}$ for $\{(2,2'$ -dipyridylamine) $\text{Cu}(\text{OH})_2\}^{2+}$ catalyzed hydrolysis of *p*-nitrophenyl acetate (**25**). This ester would not be useful as a substrate for the $\{(2,2'$ -dipyridylamine) $\text{Cu}(\text{OH})_2\}^{2+}$

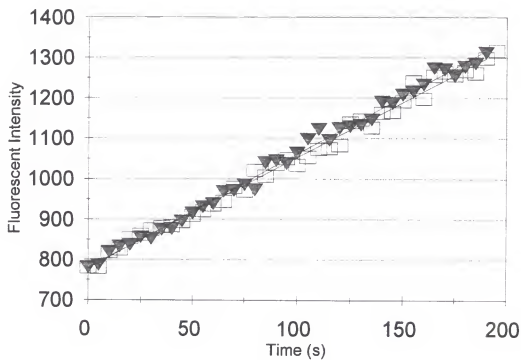


Figure 4.3
Plot of fluorescent intensity versus time (s) for hydrolysis of 2,4-dinitrobenzoic acid,
7-hydroxycoumarin ester

modified antibody because MOPC-315 has a relatively low affinity for the *p*-nitrophenyl group.^{13,37} However, investigation of **25** with the copper complex would provide insight into the complex's catalytic ability under the conditions set for the study. The *p*-nitrophenolate that is released upon hydrolysis of the ester absorbs at a wavelength of 417 nm, and the reaction is easily followed by monitoring this absorbance. Figure 4.4 shows hydrolysis of **25**.

The conditions for rate data collection were chosen according to the same criteria as the previous studies with **23**. Again, the pH was maintained at 7.0, and the temperature was selected to be 25°C. An ester concentration of 0.1 mM was selected because this resulted in a maximum absorbance of 0.922 for the release of *p*-nitrophenolate product, a value that lies within the linear range of absorbance versus time according to Beer's Law.

The rate constant for $\{(2,2'\text{-dipyridylamine})\text{Cu}(\text{OH}_2)_2\}^{2+}$ catalyzed hydrolysis of *p*-nitrophenyl acetate was determined to be $(9.4 \pm 0.4) \times 10^{-3} \text{ M}^{-1} \text{ s}^{-1}$. Figure 4.5 shows the A_{417} of *p*-nitrophenol released versus time. There was an obvious leveling off in the catalyzed rate as the reaction approached completion. The extinction coefficient of $21330 \text{ L mol}^{-1} \text{ cm}^{-1}$ for *p*-nitrophenol was obtained according to Beer's Law from a plot of absorbance at 417 nm versus *p*-nitrophenyl acetate concentration (Figure 4.6). The rate data were converted to concentration versus time, and the rate constant was extracted according to the rate expression below (Equation 4-1).

$$v = k_{\text{OH}}[\text{OH}^-][\text{Ester}] + k_{\text{cat}}[\text{CuL}][\text{Ester}] \quad (4-1)$$

where $\text{CuL} = 1$

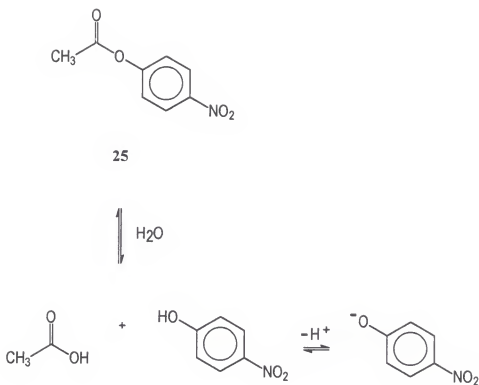


Figure 4.4
Hydrolysis of *p*-nitrophenyl acetate

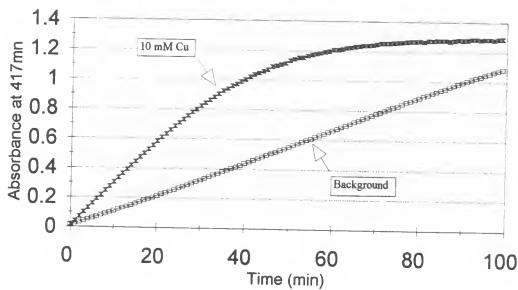


Figure 4.5
Plot of A_{417} versus time (min) for $\{(2,2'\text{-dipyridylamine})\text{Cu}(\text{OH})_2\}^{2+}$ catalyzed
hydrolysis of *p*-nitrophenyl acetate

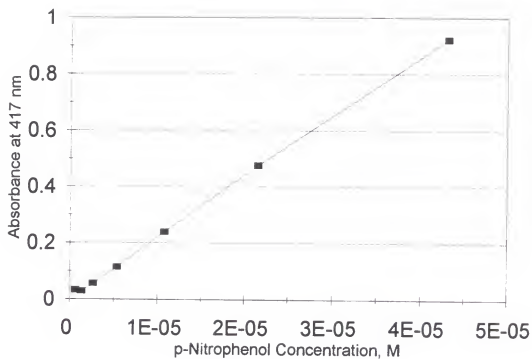


Figure 4.6
Plot of A_{417} versus concentration of *p*-nitrophenol

Specifically, the rate of the background reaction, i.e. hydrolysis of **25** in pH 7.0 buffer at 25°C, was determined and k_{OH} was obtained according to Equation 4-2.

$$v' = k_{OH}[OH^-][Ester] \quad (4-2)$$

The contribution from the background reaction was subtracted from the observed rate to give the following expression (Equation 4-3).

$$v - v' = k_{cat}[CuL][Ester] \quad (4-3)$$

Note that the water contribution is negligible. This equation can be rewritten as,

$$v'' = k_{obs}[Ester] \quad (4-4)$$

$$\text{where } k_{obs} = k_{cat}[CuL] \text{ and } [CuL] = \text{constant}$$

The catalytic rate constant was extracted from a plot of $\ln(C_x - C_i)$ versus time where C is the concentration of *p*-nitrophenol product (Figure 4.7). The derivation of this relationship is given in Appendix E. Corrections were made for the percentage of catalyst in the active form (containing a copper-coordinated hydroxide, 39%) and also for the percentage of product in the absorbing form (*p*-nitrophenolate, 43%) at pH 7.0.

The observed catalyzed rate constant is much lower than the value obtained by Chin et al., $1.6 \times 10^{-1} \text{ M}^{-1} \text{ s}^{-1}$. The reason for the discrepancy may be due to differences in experimental conditions. The conditions under which Chin et al. obtained their data are not apparent. It is difficult to interpret the results since detailed information was not provided and comparisons cannot be made.

Having characterized the ability of **1** to catalyze the hydrolysis of *p*-nitrophenyl acetate, it was necessary to find a substrate similar to this ester that MOPC-315 could

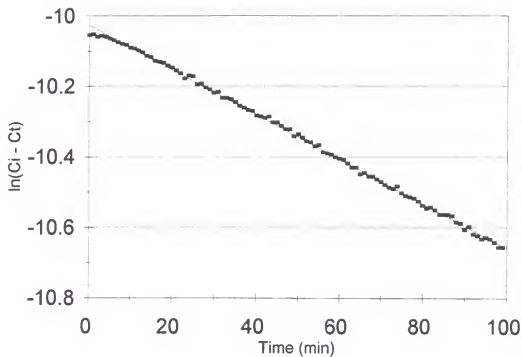


Figure 4.7

Plot of $\ln(C_\infty - C_t)$ versus time (min) for the initial rate of $\{(2,2'$ -dipyridylamine) $\text{Cu}(\text{OH}_2)_2\}^{2+}$ catalyzed hydrolysis of *p*-nitrophenyl acetate

bind. The logical choice was 2,4-dinitrophenyl acetate. This ester differs from **25** by only one nitro group, so there was a good chance it would also be susceptible to copper complex-catalyzed hydrolysis. The dinitrophenyl group allows for binding by MOPC-315, as well. On the other hand, the extra nitro group changes the reactivity of **24**. The dinitrophenyl group is more strongly electron withdrawing than the *p*-nitrophenyl group, and so 2,4-dinitrophenol is a better leaving group than *p*-nitrophenol. The result of this difference is that 2,4-dinitrophenyl acetate is more easily hydrolyzed. This is observed in the higher rate constant for the background reaction.³⁸

The rate data for hydrolysis of **24** were collected and analyzed in the same manner as for **25**. The reaction was followed by monitoring the absorbance of 2,4-dinitrophenolate product at 410 nm. The pK_a of 2,4-dinitrophenol is 3.96,³⁹ so >99% of the product should be in the phenolate form at pH 7.0. Thus, it was not necessary to make corrections for the amount of product in the absorbing form. The substrate concentration was chosen to be 0.1 mM as this value corresponded to an A_{410} reading of 0.960. The extinction coefficient of $9532 \text{ L mol}^{-1} \text{ cm}^{-1}$ was obtained from a plot of A_{410} versus 2,4-dinitrophenyl acetate concentration (Figure 4.8). The A_{410} versus time data for this reaction are shown in Figure 4.9, and a plot of $\ln(C_\infty - C_t)$ versus time, from which the catalytic rate constant was abstracted, is shown in Figure 4.10.

An interesting phenomenon is observed from a plot of $\ln(C_\infty - C_t)$ versus time if the hydrolysis of **24** is monitored past 1000 s (Figure 4.11). As demonstrated in Appendix E, a plot of $\ln(C_\infty - C_t)$ versus time for this type of second order reaction

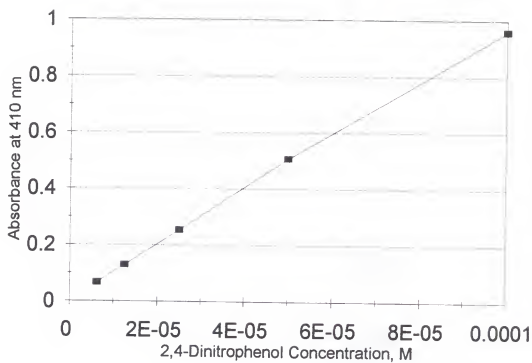


Figure 4.8
Plot of A_{410} versus concentration of 2,4-dinitrophenol

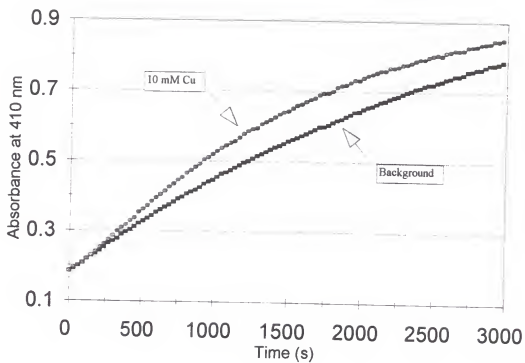


Figure 4.9
Plot of A_{410} versus time (s) for $\{(2,2'\text{-dipyridylamine})\text{Cu}(\text{OH}_2)_2\}^{2+}$ catalyzed
hydrolysis of 2,4-dinitrophenyl acetate

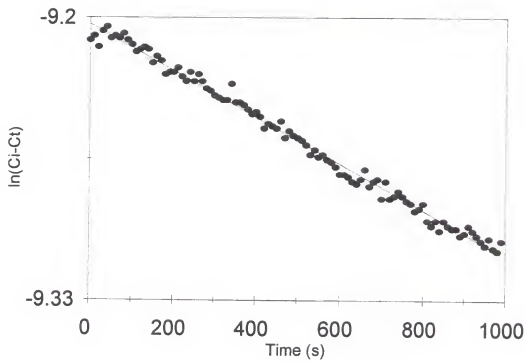


Figure 4.10

Plot of $\ln(C_\infty - C_t)$ versus time (s) for the initial rate of $\{(2,2'$ -dipyridylamine) $\text{Cu}(\text{OH}_2)_2\}^{2+}$ catalyzed hydrolysis of 2,4-dinitrophenyl acetate

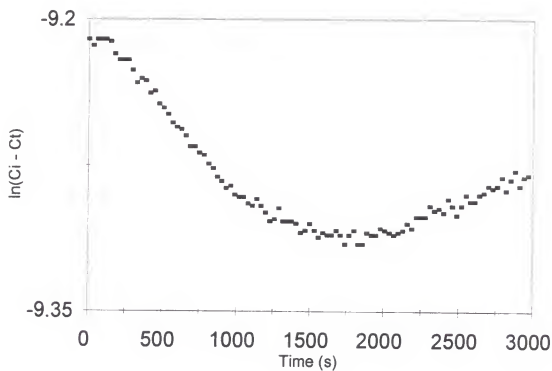


Figure 4.11

Plot of $\ln(C_\infty - C_t)$ versus time (s) for $\{(2,2'\text{-dipyridylamine})\text{-Cu}(\text{OH}_2)_2\}^{2+}$ catalyzed hydrolysis of 2,4-dinitrophenyl acetate

should give a straight line with slope equal to the negative value of the observed rate constant. If the catalyst is inhibited or consumed, the catalyzed rate should taper off until only the background rate is observed. This would be manifest in the $\ln(C_\infty - C_t)$ versus time plot as a leveling off of the negatively-sloped line into a horizontal line. What is seen in this case, however, is that the negatively-sloped line levels off and turns into a positively-sloped line. This indicates that inhibition is occurring in the uncatalyzed reaction as well as in the catalyzed reaction. Indeed, rate experiments where 2,4-dinitrophenol was added to the reaction indicate that the rate is inhibited in the presence of this product. Figure 4.12 shows a plot of rate data for hydrolysis of **24** in the presence of 0.1 mM 2,4-dinitrophenol. Clearly, the 2,4-dinitrophenol inhibits both the uncatalyzed and the catalyzed reactions, although the effect is greater on the catalyzed reaction.

The reason for this behavior is most likely due to back reaction of the liberated 2,4-dinitrophenolate ion with unstable acylated intermediates. A similar phenomenon was observed by Jencks and Gilchrist in a study of catalysis of *p*-nitrophenyl acetate hydrolysis by a series of pyridine nucleophiles.³⁸ The phenolate ion is unexpectedly reactive, relative to hydroxide ion, toward acyl-nucleophile intermediates. Presumably, phenolate ion reacts with the intermediate to push the equilibrium back toward reactants, thus decreasing the effective rate of hydrolysis. Based on this explanation, inhibition of the background reaction would not be expected. The detection of background inhibition in this case is caused by the presence of dibasic phosphate ion and possibly extraneous metal ions. What is actually being observed is

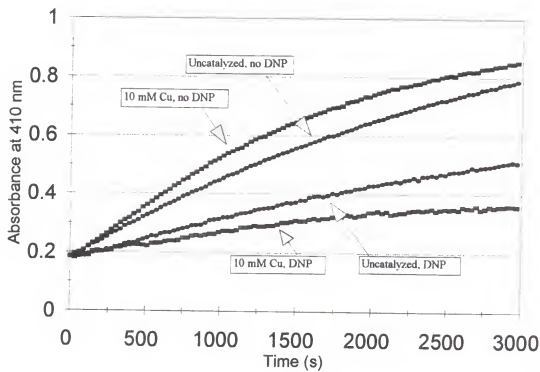


Figure 4.12

Plot of A_{410} versus time (s) for hydrolysis of 2,4-dinitrophenyl acetate in the presence of 0.1 mM 2,4-dinitrophenol

inhibition of the hydrolysis reaction catalyzed by these adventitious species. The odd behavior required that the rate constant for hydrolysis of **24** be obtained from initial rate data, i.e. data collected up to 1000 s (~31% of reaction).

The rate constant for $\{(2,2'\text{-dipyridylamine})\text{Cu}(\text{OH}_2)_2\}^{2+}$ -catalyzed hydrolysis of 2,4-dinitrophenyl acetate was found to be $(2.08 \pm 0.06) \times 10^{-2} \text{ M}^{-1} \text{ s}^{-1}$. This value is over two times the catalyzed rate constant found for *p*-nitrophenyl acetate hydrolysis. The 2,4-dinitrophenyl acetate is considered to be more activated than **25** because the product of its hydrolysis, 2,4-dinitrophenolate, has greater resonance stabilization than *p*-nitrophenolate and thus is a better leaving group. Hence, the greater rate constant for 2,4-dinitrophenyl acetate is consistent with the fact that it is a more activated ester.

It should be noted that the experimentally determined background rate constants for hydrolysis of both *p*-nitrophenyl acetate ($4.95 \pm .07 \times 10^2 \text{ M}^{-1} \text{ s}^{-1}$) and 2,4-dinitrophenyl acetate ($2.14 \pm .01 \times 10^3 \text{ M}^{-1} \text{ s}^{-1}$) were approximately fifty times values reported in the literature.³⁸ The high rates were caused by the aforementioned presence of extraneous catalysts in the reaction solution. Dibasic phosphate ion is known to catalyze the hydrolysis of *p*-nitrophenyl acetate,⁴⁰ and in this set of experiments, it was present at a relatively high concentration. It is also possible that secondary metal ions were responsible for the high rates since an exhaustive removal of these ions was not performed. In any case, the high background rates should not have an effect on the catalyzed rate constants because these constants were calculated based on the difference between catalyzed and background rates. In essence, the extraneous catalysis was subtracted out prior to catalyzed rate constant determination.

Antibody Catalyzed Reactions

The rate data for hydrolysis of **24** in the presence of dipyridylamine-functionalized Fab were collected and analyzed in the same manner as described for the $\{(2,2'\text{-dipyridylamine})\text{Cu}(\text{OH})_2\}^{2+}$ catalyzed experiments. However, in this case, the catalyst concentration was at least a thousand times lower. Initially, the metalloantibody rate studies were carried out by incubating 1 μM dipyridylamine-linked Fab with 100 μM copper ion at pH 7.0 for approximately 3 min prior to reaction with the ester. The A_{410} versus time results, shown in Figure 4.13, indicate that the dipyridylamine-functionalized Fab causes rate acceleration both in the presence and in the absence of copper ion. The data also suggest that the influence of the metalloantibody on reaction rate is not caused by a proximity effect. Rather, the metalloantibody-catalyzed results appear to be no more than an added effect from the non-metalated antibody and the copper ion in solution. If the catalyst were acting as anticipated, the rate enhancement would be much greater.

Solubility studies of copper(II) ion in various solvents were performed. The results indicate that copper precipitates in phosphate buffer at a range of pH values including 7.0, possibly as copper hydroxide or copper phosphate. It follows that no copper was bound by dipyridylamine-linked Fab under the same conditions due to precipitation and, because of this, no proximity effect was observed with the 'metalloantibody' rate experiments. In essence, the catalyst was not present, and thus the anticipated rate enhancement was not observed.

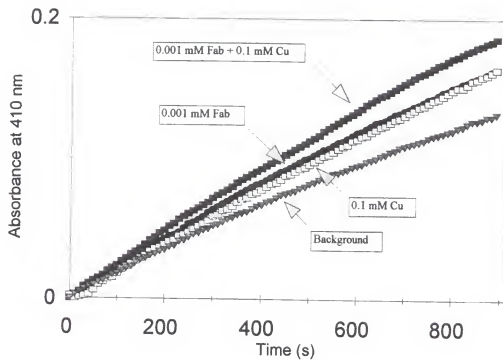


Figure 4.13
Plot of A_{410} versus time (s) for dipyrldiamine-functionalized Fab catalyzed hydrolysis of 2,4-dinitrophenyl acetate

A new strategy for metallation of the Fab was attempted. Rather than incubating antibody with copper ion at pH 7.0, as done previously, the antibody solution was dialyzed to pH 4.9 before copper solution was added. In pH 4.9 MES buffer, the copper ion is completely soluble and thus theoretically able to form a complex with dipyridylamine-linked Fab. The pH was then raised back to 7.0 so that the copper complex catalyst would be in its active form.

The rate data for hydrolysis of 2,4-dinitrophenyl acetate in the presence of pH 4.9 metallated Fab are shown in Figure 4.14. The pH 4.9 metallated antibody had no effect on the rate of the reaction; even the rate enhancement observed with the non-metallated version was removed. Interestingly, the small amount of rate enhancement demonstrated by unmodified IgA was also eliminated by metallation. It appears as though the metallation procedure damaged the antibody in some way. It is possible that the decrease in pH was drastic enough to irreversibly denature the protein.

Although it was not possible to obtain rate data for a genuine metalloabzyme, the dipyridylamine-linked Fab rate enhancement was analyzed. The rate constant for dipyridylamine-modified Fab catalyzed hydrolysis was determined in the same manner as for the $\{(2,2'\text{-dipyridylamine})\text{Cu}(\text{OH})_2\}^{2+}$ catalyzed reaction, from a plot of $\ln(C_\infty - C_t)$ versus time (Figure 4.15). The value of $(4.3 \pm 0.4) \times 10 \text{ M}^{-1} \text{ s}^{-1}$ indicates that the antibody is more efficient at catalyzing hydrolysis of 2,4-dinitrophenyl acetate than the copper complex. However, the mechanism by which the antibody works is unknown.

For purposes of comparison, a catalytic rate constant consistent with the Michaelis-Menten equation was estimated for Fab catalyzed hydrolysis of 2,4-

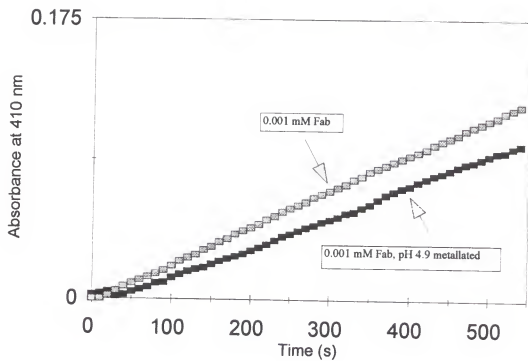


Figure 4.14

Plot of A_{410} versus time (s) for hydrolysis of 2,4-dinitrophenyl acetate in the presence of pH 4.9 metallated dipyrldiamine-functionalized Fab

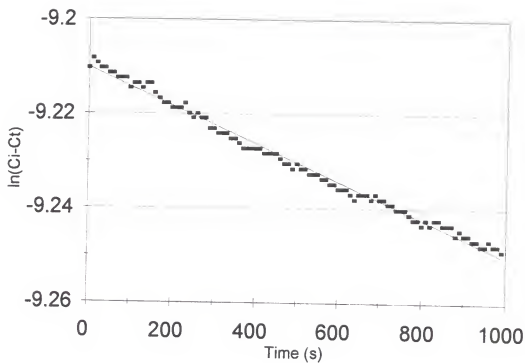


Figure 4.15

Plot of $\ln(C_{\infty} - C_t)$ versus time (s) for dipyrldylamine-functionalized Fab catalyzed hydrolysis of 2,4-dinitrophenyl acetate

dinitrophenyl acetate. Since the ester was present in one hundred times excess of the antibody, it was assumed that the antibody binding site (i.e. "active site") was saturated with substrate. It follows that the rate measured under these conditions is the maximum rate that the antibody is capable of. According to Michaelis-Menten theory, the maximum rate is equal to the catalytic rate constant multiplied by enzyme concentration:

$$V_{\max} = k_{\text{cat}}[E_T] \quad (4-5)$$

Thus, the first order catalytic rate constant was determined by dividing the observed rate by the total antibody concentration. The resulting k_{cat} was 0.24 min^{-1} , a value that falls within the range of rate constants reported for catalytic antibodies.^{1,4} To determine the second order rate constant (k_{cat}/K_M) according to Michaelis-Menten theory, a K_M value was necessary. This value was taken to be the dissociation constant for 2,4-dinitrophenyl acetate binding to MOPC-315. Although this particular dissociation constant is not known, the K_D values for MOPC-315 binding of many other 2,4-dinitrophenyl substituted species have been determined.¹³ Based on these data, the K_M for 2,4-dinitrophenyl binding was taken to be $84 \times 10^{-5} \text{ M}$ (the K_D for a structurally similar species), and the second order rate constant was calculated as $4.7 \times 10 \text{ M}^{-1} \text{ s}^{-1}$. This value indicates that the antibody causes rate enhancement of approximately 2500 times that which dipyridylamine alone is capable of. This rate enhancement is similar to that observed by Pollack et al. for imidazole-functionalized MOPC-315.^{11c}

EPR Characterization of 1

The complex **1** used in kinetic studies was characterized using EPR. Data were obtained for **1**, copper(II) nitrate, and **1** in the presence of excess dipyridylamine ligand (Figure 4.16). The $\{(2,2'\text{-dipyridylamine})\text{Cu}(\text{OH})_2\}^{2+}$ spectrum, $g_{\perp} = 2.06$ and $g_{\parallel} = 2.30$, is distinctly different from the spectrum for copper(II) nitrate, $g_{\perp} = 2.08$ and $g_{\parallel} = 2.41$. Hyperfine coupling is apparent in the spectrum of **1** in the presence of excess ligand. The species present in this solution is likely the symmetrical bis-dipyridylamine complex.

Spectra were gathered for **1** at pH values of 4.0, 7.0, and 8.0. Each spectrum was unique, indicating the presence of different species (Figure 4.17). At pH 4.0, the complex is in the diaqua form. At pH 8.0, it should have one water and one hydroxide ligand as the pK_a for the first water is 7.2. The spectra are consistent with the presence of these two forms. There is likely to be dimerization of the complex at pH 8.0 which would allow for antiferromagnetic coupling between the copper ions. This is manifest in the spectrum as a relatively low signal to noise ratio. At pH 7.0 there is a mixture of the diaqua and monoaqua forms. As a result, the spectral peaks are spread out relative to those at the other pH values.

These experiments established a method for differentiating between the copper-dipyridylamine complex and other forms of copper ion in solution. It should be possible to use EPR to determine if the copper(II) ion is bound to the dipyridylamine in the antibody similar to the way Nakayama and Schultz did,²⁸

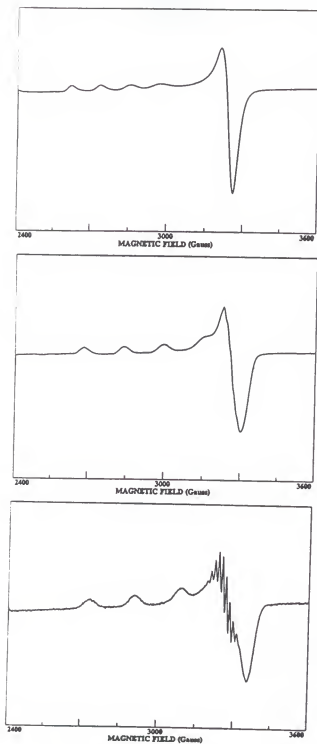


Figure 4.16
EPR spectra for copper(II) nitrate (top), **1** (middle), and **1** with excess dipyrildamine (bottom)

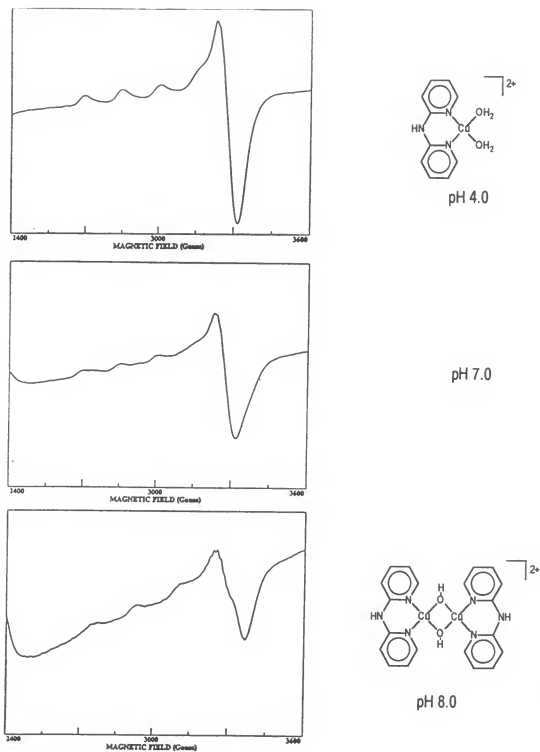


Figure 4.17
EPR spectra for **1** at various pH values

provided the concentration is high enough for the instrument to detect. Unfortunately, the amount of antibody used in this study was not enough to investigate using EPR, so another approach to the problem was required.

Experimental Methods

General Procedures

Fluorescence spectra were recorded on a SPEX Fluorolog spectrophotometer, and absorbance spectra were recorded on a Nicolet 9420 spectrophotometer. Proton NMR spectra were recorded at 300 MHz on a General Electric QE-300 spectrometer. Chemical shifts are reported in parts per million; the residual solvent peak was used as an internal standard. Electron Paramagnetic Resonance spectra were recorded on a Bruker ER 200D spectrometer and were obtained using solutions of sample frozen in liquid nitrogen. Elemental analysis (C,H,N) was performed by the University of Florida Department of Chemistry Analytical Services. Reagents and solvents were of analytical grade and used as supplied with the following exceptions: Ethanol was distilled from magnesium metal. The compound 2,2'-dipyridylamine was recrystallized from benzene. The compounds *p*-nitrophenyl acetate, *p*-nitrophenol, 2,4-dinitrophenyl acetate, and 2,4-dinitrophenol were dried in a vacuum oven. Water was purified in a Barnstead nanopure water system such that resistance was no less than 17 megaohms.

Synthesis of 2,4-Dinitrobenzoic Acid, 7-Hydroxycoumarin Ester (23)

The substrate 2,4-dinitrobenzoic acid, 7-hydroxycoumarin ester₂ (2.12g, 58%) was prepared according to a method described by Pollack et al.:^{11b} ¹H NMR (DMSO-

δ 8.93 (d, $J = 2.2$ Hz, 1H), 8.77 (dd, $J = 2.2, 8.4$ Hz, 1H), 8.44 (d, $J = 8.4$ Hz, 1H), 8.11 (d, $J = 9.6$ Hz, 1H), 7.88 (d, $J = 8.5$ Hz, 1H), 7.47 (d, $J = 2.1$ Hz, 1H), 7.33 (dd, $J = 2.2, 8.5$ Hz, 1H), 6.53 (d, $J = 9.6$ Hz, 1H).

Kinetic Measurements and Data Analysis

Fluorometric measurements for the hydrolysis of 2,4-dinitrobenzoic acid, 7-hydroxycoumarin ester were measured on a SPEX Fluorolog with excitation at 355 nm and emission at 461 nm. Reactions were performed in a total of 3.00 mL of 0.1 M phosphate buffer, pH 7.0. A stock solution of the ester substrate was prepared in dimethyl sulfoxide to minimize pre-experiment hydrolysis. The cuvettes used were 1 cm methacrylate cells.

The rates for hydrolysis of *p*-nitrophenyl acetate were measured by absorbance changes at 417 nm on a Nicolet 9420 spectrophotometer. The rates for hydrolysis of 2,4-dinitrophenyl acetate were measured by absorbance changes at 410 nm on the same instrument. The bandwidth was 4.00 nm. Reactions other than those involving antibody were performed in a total of 3.00 mL of 0.1 M phosphate buffer, pH 7.0 in a quartz cuvette. The 25°C temperature was maintained using a circulating water bath. Stock solutions of the esters were prepared in acetonitrile. Rate data were collected until hydrolysis of total substrate was 75% complete for *p*-nitrophenyl acetate hydrolysis and 31% complete for 2,4-dinitrophenyl acetate hydrolysis. The concentration of $\{(2,2'\text{-dipyridylamine})\text{Cu}(\text{OH})_2\}^{2+}$ was 10 mM, and the initial concentration of ester was 0.1 mM. The observed rates were corrected for the

uncatalyzed rate of hydrolysis. Catalytic rate constants were determined from a plot of $\ln(C_{\infty} - C_t)$ versus time, as discussed previously.

The rates for hydrolysis of 2,4-dinitrophenyl acetate in the presence of antibody were also measured by absorbance changes at 410 nm on a Nicolet 9420 spectrophotometer. Reactions were performed in a total of 150 μL of 0.1 M phosphate buffer, pH 7.0 in a quartz cuvette. Rate data were collected until hydrolysis of total substrate was 36% complete. The initial concentration of ester was 0.1 mM. In one set of experiments, 1 μM dipyridylamine-functionalized Fab was incubated with 100 μM copper(II) chloride at 25°C in pH 7.0 phosphate buffer for ~3 min and then allowed to react with 2,4-dinitrophenyl acetate. The other set of experiments involved incubation of dipyridylamine-functionalized Fab with equimolar copper(II) nitrate in pH 4.9 MES buffer followed by dialysis of the solution up to pH 7.0 with phosphate buffered saline prior to reaction with ester. Again, the observed catalytic rates were corrected for the uncatalyzed rate of hydrolysis. Catalytic rate constants were determined from a plot of $\ln(C_{\infty} - C_t)$ versus time.

Synthesis of (2,2'-Dipyridylamine)copper(II) Chloride

To a stirred solution of copper(II) chloride (1.06 g, 7.89 mmol) in water (20 mL) was added a solution of 2,2'-dipyridylamine (1.35 g, 7.89 mmol) in methanol (60 mL). The resulting green mixture was stirred at 25°C for 24 h and then filtered. Dark green needle-like crystals of product formed in the filtrate: Anal. Calcd for $\text{C}_{10}\text{H}_9\text{Cl}_2\text{CuN}_3$: C, 39.30; H, 2.97; N, 13.75. Found: C, 39.33; H, 2.94; N, 13.80.

UV-vis λ_{max} : pH 6.0, 346.0 nm; pH 7.0, 342.4 nm; pH 7.5, 341.2 nm; pH 8.0, 340.8 nm.

Synthesis of (2,2'-Dipyridylamine)copper (II) Bis-aqua Complex (1)

To a stirred solution of copper(II) chloride (26.9 mg, 0.20 mmol) in water (10 mL) was added a solution of 2,2'-dipyridylamine (34.2 mg, 0.20 mmol) in dimethyl sulfoxide (10 mL). The kelly green solution of **1** was analyzed using EPR, $g_{\perp} = 2.06$, $g_{\parallel} = 2.31$.

Conclusions

The rate constant for $\{(2,2'\text{-dipyridylamine})\text{Cu}(\text{OH}_2)_2\}^{2+}$ catalyzed hydrolysis of 2,4-dinitrophenyl acetate was determined to be $(2.08 \pm 0.06) \times 10^{-2} \text{ M}^{-1} \text{ s}^{-1}$. This value is greater than the catalyzed rate constant for *p*-nitrophenyl acetate, $(9.4 \pm 0.4) \times 10^{-3} \text{ M}^{-1} \text{ s}^{-1}$, as expected. However, there were many unanticipated observations encountered in the kinetic studies involving **1**. The complex showed no catalytic activity toward hydrolysis of **23**, and the catalytic rate constant for hydrolysis of **25** was found to be much lower than the value reported by Chin et al. These results may be influenced by changing the experimental conditions under which the reaction is run. For example, altering the buffer system, or even using a solvent other than a buffer and controlling the pH of the reaction by addition of acid or base, should affect the results.

Dipyridylamine-functionalized MOPC-315 Fab was shown to catalyze hydrolysis of 2,4-dinitrophenyl acetate, the rate constant being $(4.3 \pm 0.4) \times 10^{-1} \text{ M}^{-1} \text{ s}^{-1}$. However, the antibody/copper(II) solution did not show rate enhancement consistent

with a proximity effect due to $\{(2,2'\text{-dipyridylamine})\text{Cu}(\text{OH})_2\}^{2+}$ catalyzed hydrolysis. These data are in agreement with results of a study of 1,4,8,11-tetraazacyclotetradecane-labeled MOPC-315 Fab conducted by Nakayama and Schultz.²⁸ The reason for the lack of metalloantibody activity is apparently insufficient binding of copper(II) ion. Further study should be directed at determining the best conditions for metal binding to occur.

The question arises as to how the functionalized antibody causes rate acceleration. The unmodified MOPC-315 Fab caused modest rate enhancement, presumably due to stabilizing interactions between amino acid side chains and a high energy species along the hydrolysis reaction pathway. Incorporation of dipyrldylamine near the binding site had a distinct effect on the rate of the reaction. The dipyrldylamine may act as a nucleophile and attack the carbonyl carbon of the ester directly. Or, it could act as a general base and activate a water molecule to attack the ester. Differentiation between these possibilities would involve attempting to observe the acyl-dipyrldylamine intermediate that should be formed if the nucleophilic hypothesis is correct, a difficult task further complicated by the fact that dipyrldylamine is attached to a 55,000 amu protein. It would be very interesting to observe the effect of formation of the copper complex in the antibody binding site because the proposed mechanism for copper complex catalyzed hydrolysis is a bifunctional one. Apparently, the copper complex acts via both Lewis acid and metal hydroxide mechanisms (Figure 1.7).

An essential step to take at this point is analysis of Fab catalyzed hydrolysis according to Michaelis-Menten kinetics. The Michaelis-Menten parameters k_{cat} and K_M were estimated based on the assumption of saturation conditions, but a more rigorous treatment, including measurement of the rate of antibody catalyzed hydrolysis at a range of different substrate concentrations, should be performed. The Michaelis-Menten kinetic theory of enzyme catalysis is used to explain the behavior of enzymes and other abzymes.^{1,4,11} It assumes the formation of an enzyme-substrate complex, which is a valid assumption for antibody catalysis, as well. Certainly, if the antibody has a substantial effect on the reaction (as opposed to the dipyridylamine alone causing rate enhancement) the rate data should conform to the Michaelis-Menten equation. Under the same conditions as for the antibody catalyzed reaction, 2,2'-dipyridylamine alone was shown to have no effect on the rate of hydrolysis, and, as noted previously, adherence to Michaelis-Menten kinetics is expected.

CHAPTER 5 CONCLUSION

Catalytic antibodies can be considered synthetic enzymes because they are man-made, or rather man-induced, but still contain all the complexity of the relatively large protein catalysts. There are many enzymes that act as catalysts in conjunction with metals, as mentioned earlier. Because of the analogy between catalytic antibodies and enzymes, the study of antibodies as catalysts will not be complete until there has been more extensive investigation of the potential for metalloantibody catalysis. A current emphasis in abzyme research is on increasing the rate enhancement induced by antibodies. Incorporation of metals is one possible way to do this, and this work was designed to contribute to that effort.

A method for preparing a metal complex-containing hapten to be used to elicit a metalloabzyme was investigated. Much of the synthetic pathway was worked out. All that is yet to be done is synthesis of a phosphate model species that will not displace the dipyridylamine ligand on platinum. This might be accomplished by using a phosphate compound that contains one oxygen donor atom and one sulfur donor atom. The resulting hapten might then be used to elicit antibodies that would be specific for a high energy species along the reaction pathway of metal complex-catalyzed hydrolysis. The resulting antibodies would very likely enhance the rate of the hydrolysis reaction even further than is observed for the metal complex alone.

Synthesis of transition state model complexes can be lengthy and difficult, a point demonstrated by this work. Indeed, the synthesis of an appropriate model complex is often the limiting factor in abzyme production. Abzymes that catalyze reactions based solely on transition state stabilization cause rate enhancements with a limit of approximately 10^4 .⁴¹ An important step to take at this point in catalytic antibody development is to surpass rate accelerations obtained by transition state model-induced abzymes by enhancing the transition state stabilization interactions. The present work, combination of transition state stabilization with incorporation of a metal complex cofactor, is one example of this. There are others, as well. Stewart et al.⁴² have investigated existing abzymes in order to determine their mechanism of action. With this information, the binding site could be altered to maximize the stabilization induced by the antibody. The two major methods by which this is accomplished are site-directed mutagenesis⁴² and chemical modification¹¹ of binding site residues. It seems that an antibody is only capable of a certain level of rate enhancement via transition state stabilization, and outside manipulation is necessary to further enhance abzyme catalysis.

The other method of metalloabzyme preparation that was investigated was the semi-synthetic procedure. This procedure was used to prepare an antibody with a dipyridylamine group linked near the binding site. The ability of this antibody to catalyze hydrolysis of 2,4-dinitrophenyl acetate in the presence and absence of copper(II) ion was assessed. The functionalized antibody was found to cause rate enhancement. However, the metal ion was not bound by the dipyridylamine group,

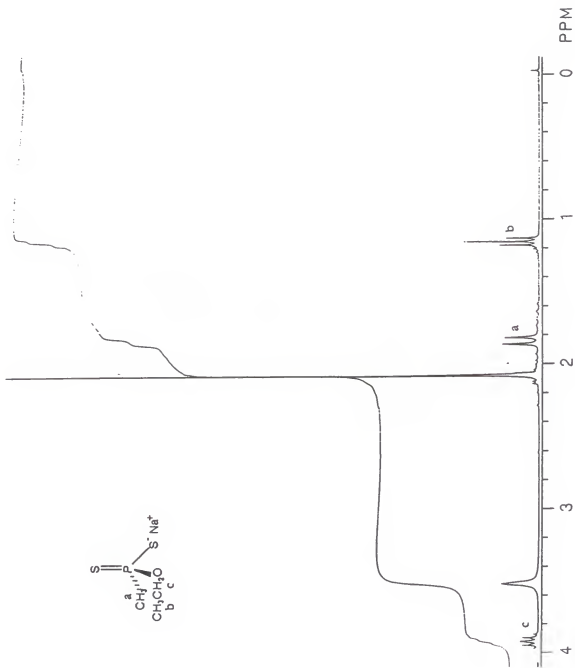
and thus the anticipated rate enhancement resulting from a proximity effect was not observed. The optimal conditions for formation of a metal complex must be further investigated in order to determine whether a metal complex situated near the binding site of the MOPC-315 antibody can cause rate enhancement for hydrolysis of bound substrate. Specifically, the conditions under which the antibody can be metallated without causing damage to amino acid residues must be found. A gradual change in the pH of the solution appears to disrupt the non-covalent interactions of the protein. Thus, a milder protocol is necessary.

An appropriate direction for metalloabzyme research to take would be to attempt an increase in the rate acceleration exhibited by catalytic antibodies by combining two different strategies. Iverson, Roberts. et al. constructed an antibody with a coordination site for metals in the antigen binding pocket.⁴³ This method of development of metalloantibodies could be taken a step further. For example, one could take an existing transition state model-induced abzyme that exhibits decent rate enhancement and, through site-directed mutagenesis, introduce a metal binding site near the antigen (substrate) binding site. The metal might cause further stabilization of the intermediate species and induce rate acceleration. This approach exemplifies another way in which transition state stabilization could be expanded to include a metal complex cofactor. A semi-synthetic antibody could be modified in an analogous manner to give similar results.

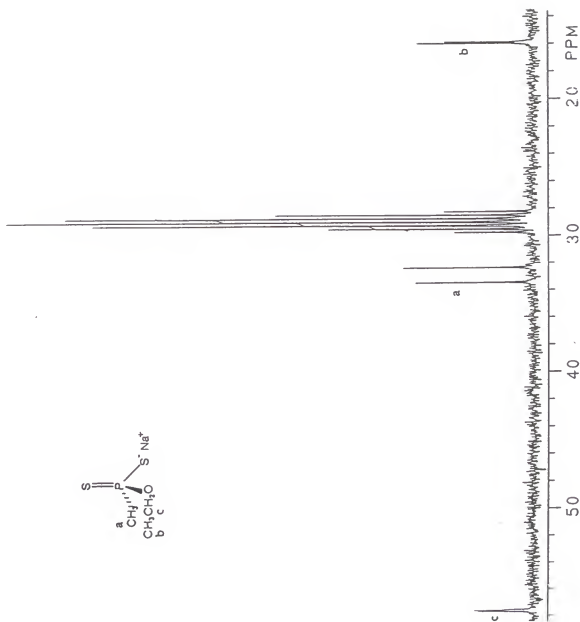
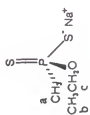
APPENDIX A
ATTEMPTED FUNCTIONALIZATION OF 2,2'-DIPYRIDYLAMINE



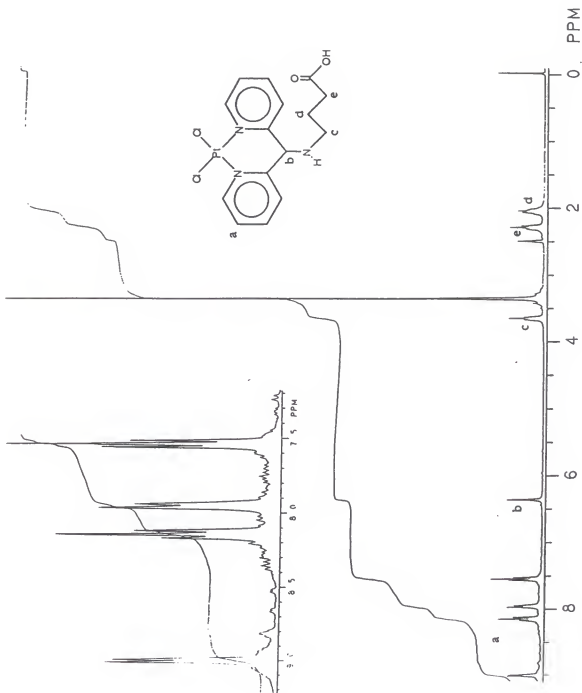
APPENDIX B
PROTON NMR SPECTRUM OF 4 IN ACETONE- d_6



APPENDIX C
CARBON NMR SPECTRUM OF **4** IN ACETONE- d_6



APPENDIX D
PROTON NMR SPECTRUM OF **6** IN DMSO-d₆



APPENDIX E
DERIVATION OF THE EXPRESSION $\ln(P_t - x) = -k_{obs}t + \ln(P_t)$

The equation $v'' = k_{\text{obs}}[\text{Ester}]$ can be written as $\frac{dx}{dt} = k_{\text{obs}}(E_0 - x)$
 where x = amount of Ester reacted or amount of Product released.

$$\frac{dx}{dt} = k_{\text{obs}}(E_0 - x)$$

or

$$\frac{dx}{(E_0 - x)} = k_{\text{obs}} dt$$

$$\int \frac{dx}{(E_0 - x)} = \int k_{\text{obs}} dt \quad \text{integrating both sides...}$$

$$-\ln(E_0 - x) = k_{\text{obs}} t + \text{const.}$$

When $t = 0$, $x = 0$ and

$$\text{const.} = -\ln(E_0)$$

$$-\ln(E_0 - x) = k_{\text{obs}} t - \ln(E_0) \quad \text{or}$$

$$\ln(E_0 - x) = -k_{\text{obs}} t + \ln(E_0)$$

Since the initial amount of Ester E_0 is equal to the maximum amount of Product Pr formed, this can be written...

$$\ln(Pr - x) = -k_{\text{obs}} t + \ln(Pr)$$

A plot of $\ln(Pr - x)$ versus t will give a slope of $-k_{\text{obs}}$ and a y-intercept of $\ln Pr$.

REFERENCES

1. (a) Green, B. S. *Adv. Biotechnol. Processes* **1989**, *11*, 359. (b) Shokat, K. M.; Schultz, P. G. *Annu. Rev. Immunol.* **1990**, *8*, 335. (c) Benkovic, S. J. *Annu. Rev. Biochem.* **1992**, *61*, 29. (d) Pankit, U. K. *Recl. Trav. Chim. Pays-Bas* **1993**, *112*, 431. (e) Schultz, P. G.; Lerner, R. A. *Acc. Chem. Res.* **1993**, *26*, 391. (f) Stewart, J. D.; Benkovic, S. J. *Chem. Soc. Rev.* **1993**, 213. (g) Hilhorst, R. *Anal. Chim. Acta* **1993**, *279*, 129. (h) Blackburn, G. M.; Wentworth, P. *Chemistry and Industry* **1994**, 338. (i) Suzuki, H. *J. Biochem.* **1994**, *115*, 623. (j) Hilvert, D. *Curr. Opin. Struct. Biol.* **1994**, *4*, 612.
2. (a) Lehn, J. M. *Science* **1985**, *227*, 849. (b) Schmidtchen, F. P. *Top. Curr. Chem.* **1986**, *132*, 101. (c) Breslow, R. *Adv. Enzymol.* **1986**, *58*, 1. (d) Rebek, J. *Science* **1987**, *235*, 1478. (e) Werber, M. M. *Adv. Clin. Enzymol.* **1987**, *5*, 123. (f) Cram, D. J. *Angew. Chem. Int. Ed. Engl.* **1988**, *27*, 1009. (g) Lehn, J. M. *Angew. Chem. Int. Ed. Engl.* **1988**, *27*, 89. (h) Rebek, J. *Acc. Chem. Res.* **1990**, *23*, 399.
3. (a) Johnson, K. A.; Benkovic, S. J. *Enzymes* **1990**, *19*, 159. (b) Clarke, A. R. *Trends Biochem. Sci.* **1989**, *14*, 145.
4. Lerner, R. A.; Benkovic, S. J.; Schultz, P. G. *Science* **1991**, *252*, 659.
5. (a) Pauling, L. *Chem. Eng. News* **1946**, *24*, 1375. (b) Pauling, L. *Nature* **1948**, *161*, 707.
6. Jencks, W. P. In *Catalysis in Chemistry and Enzymology*, New York: McGraw-Hill, 1969, 288.
7. Kohler, G.; Milstein, C. *Nature* **1975**, *256*, 495.
8. (a) Wolfenden, R. *Annu. Rev. Biophys. Bioeng.* **1976**, *5*, 271. (b) Stark, G. R.; Bartlett, P. A. *Pharmac. Ther.* **1983**, *23*, 45. (c) Wolfenden, R. *Transition States Biochem. Processes* **1978**, 555. (d) Wolfenden, R.; Frick, L. J. *Protein Chem.* **1986**, *5*, 147. (e) Bartlett, P. A. *Colloq. Ges. Biol. Chem.* **1988**, *39*, 86. (f) Morgan, B. P.; Scholtz, J. M.; Ballinger, M. D.; Zipkin, I. D.; Bartlett, P. A. *J. Am. Chem. Soc.* **1991**, *113*, 297. (g) Phillips, M. A.; Kaplan, A. P.; Rutter, W. J.; Bartlett, P. A. *Biochemistry* **1992**, *31*, 959.

9. Pollack, S. J.; Jacobs, J. W.; Schultz, P. G. *Science* **1986**, *234*, 1570.
10. Tramontano, A.; Janda, K. D.; Lerner, R. A. *Science* **1986**, *234*, 1566.
11. (a) Pollack, S. J.; Nakayama, G. R.; Schultz, P. G. *Science (Wash DC)* **1988**, *242*, 1038. (b) Pollack, S. J.; Nakayama, G. R.; Schultz, P. G. *Methods Enzymol.* **1989**, *178*, 551. (c) Pollack, S. J.; Schultz, P. G. *J. Am. Chem. Soc.* **1989**, *111*, 1929. (d) Pollack, S. J. *Ph.D. Dissertation*; University of California, Berkeley: Berkeley, CA, 1990.
12. (a) Eisen, H. N.; Simms, E. S.; Potter, M. *Biochemistry* **1968**, *7*, 4126. (b) Goetzl, E. J.; Metzger, H. *Biochemistry* **1970**, *9*, 1267. (c) Underdown, B. J.; Simms, E. S.; Eisen, H. N. *Biochemistry* **1971**, *10*, 4359. (d) Inbar, D.; Hochman, J.; Givol, D. *Proc. Nat. Acad. Sci. USA* **1972**, *69*, 2659. (e) Hochman, J.; Inbar, D.; Givol, D. *Biochemistry* **1973**, *12*, 1130. (f) Schechter, I.; Ziv, E.; Licht, A. *Biochemistry* **1976**, *15*, 2785. (g) Zidovetski, R.; Sicht, A.; Pecht, I. *Proc. Natl. Acad. Sci. USA* **1979**, *76*, 5848.
13. Haselkorn, D.; Friedman, S.; Givol, D.; Pecht, I. *Biochemistry* **1974**, *13*, 2210.
14. (a) Givol, D.; Wilchek, M. *Methods Enzymol.* **46**, 479. (b) Givol, D.; Strausbauch, P. H.; Hurwitz, E.; Wilchek, M.; Haimovich, J.; Eisen, H. N. *Biochemistry* **1971**, *10*, 3461. (c) Strausbauch, P. H.; Weinstein, Y.; Wilchek, M.; Shaltiel, S.; Givol, D. *Biochemistry* **1971**, *10*, 4342.
15. Stryer, L. *Biochemistry*, 3rd ed.; W. H. Freeman: New York, 1988.
16. (a) Chin, J.; Jubian, V. *J. Chem. Soc., Chem. Commun.* **1989**, 839. (b) Chin, J.; Jubian, V.; Mrejen, K. *J. Chem. Soc., Chem. Commun.* **1990**, 1326. (c) Chin, J. *Acc. Chem. Res.* **1991**, *24*, 145.
17. (a) Jencks, W. P. *J. Am. Chem. Soc.* **1964**, *86*, 837. (b) Menger, F. M.; Ladika, M. *J. Am. Chem. Soc.* **1987**, *109*, 3145.
18. Schwabacher, A. W.; Weinhouse, M. I.; Auditor, M. M.; Lerner, R. A. *J. Am. Chem. Soc.* **1989**, *111*, 2344.
19. Reardan, D. T.; Meares, C. F.; Goodwin, D. A.; McTigue, M.; David, G. S.; Stone, M. R.; Leung, J. P.; Bartholomew, R. M.; Frincke, J. M. *Nature (London)* **1985**, *316*, 265.
20. Iverson, B. L.; Lerner, R. A. *Science* **1989**, *243*, 1184.
21. (a) Kinnear, A. M.; Perren, E. A. *J. Chem. Soc.* **1952**, 3437. (b) Newallis, P. E.; Chupp, J. P.; Groenweghe, L. C. D. *J. Org. Chem.* **1962**, *27*, 3829. (c)

- Chupp, J. P.; Newallis, P. E. *J. Org. Chem.* **1962**, *27*, 3832. (d) Grishina, O. N.; Bezzubova, L. M. *Izv. Akad. Nauk SSSR Ser. Khim.* **1966**, 1617. (e) Kosolapoff, G. M.; Maier, L. *Organic Phosphorus Compounds*; Wiley-Interscience: New York, 1976. (f) Andreev, N. A.; Grishana, O. N. *Zh. Obshch. Khim.* **1982**, *52*, 1785. (g) Navech, J.; Majoral, J. P.; Kraemer, R. *Tetrahedron Lett.* **1983**, *24*, 5885. (h) Andreev, N. A.; Grishana, O. N. *Zh. Obshch. Khim.* **1984**, *54*, 1533.
22. (a) Marcellis, A. T. M.; Van der Veer, J. L.; Zwetsloot, J. C. M.; Reedijk, J. *Inorg. Chim. Acta* **1983**, *78*, 195. (b) Osa, T.; Hino, H.; Fujieda, S.; Shiiro, T.; Kono, T. *Chem. Pharm. Bull.* **1986**, *34*, 3563. (c) Newkome, G. R.; Theriot, K. J.; Fronczek, R. R.; Villar, B. *Organometallics* **1989**, *8*, 2513.
 23. Szabo, K.; Menn, J. J. *J. Agric. Food Chem.* **1969**, *17*, 863.
 24. Borch, R. F.; Bernstein, M. D.; Durst, H. D. *J. Am. Chem. Soc.* **1971**, *93*, 2897.
 25. Erickson, L. E.; McDonald, J. W.; Howie, J. K.; Clow, R. P. *J. Am. Chem. Soc.* **1968**, *90*, 6371.
 26. Hoffmann, F. W.; Kagan, B.; Canfield, J. H. *J. Am. Chem. Soc.* **1959**, *81*, 148.
 27. Kabachnik, M. I.; Golubeva, E. I.; Paikin, D. M.; Shabanova, M. P.; Gamper, N. M.; Efimova, L. F. *Zh. Obshch. Khim.* **1958**, *29*, 1671.
 28. Nakayama, G. R.; Schultz, P. G. In *Catalytic Antibodies, Ciba Foundation Symposium 159*; Wiley: Chicester, 1991; p. 72 - 90.
 29. (a) Creighton, D. J.; Sigman, D. S. *J. Am. Chem. Soc.* **1971**, *93*, 6314. (b) Akkaya, E. U.; Czarnik, A. W. *J. Am. Chem. Soc.* **1988**, *110*, 8553.
 30. (a) Song, L.; Trogler, W. C. *J. Organomet. Chem.* **1993**, *452*, 271. (b) McDevitt, M. R.; Ru, Y.; Addison, A. W. *Transition Met. Chem.* **1993**, *18*, 197.
 31. Roitt, I.; Brostoff, J.; Male, D. *Immunology*, 1st ed.; Gower Medical: London, 1985.
 32. (a) Abel, C. A.; Grey, G. M. *Biochemistry* **1968**, *7*, 2682. (b) Warner, N. L.; Marchalonis, J. J. *J. Immunol.* **1972**, *109*, 657. (c) Wims, L. A.; Sharon, J.; Newman, B.; Kabat, E. A.; Morrison, S. L. *Molec. Immunol.* **1985**, *22*, 1379. (d) Weltzin, R.; Lucia-Jandris, P.; Fields, B. N.; Kraehenbuhl, J. P.; Neutra, M. R. *J. Cell Biol.* **1989**, *108*, 1673.

33. (a) Cossar, B. C.; Fournier, J. O.; Fields, D. L.; Reynolds, D. D. *J. Org. Chem.* **1962**, *27*, 93. (b) Urquhart, G. G.; Gates, J. W., Jr.; Connor, R. *Organic Syntheses* **1955**, *C. V. 3*, 363. (c) Mori, K.; Nakamura, Y. *J. Org. Chem.* **1969**, *34*, 4170. (d) Djerassi, C.; Gorman, M.; Markley, F. X.; Oldenburg, E. B. *J. Am. Chem. Soc.* **1955**, *77*, 568. (e) Beretta, E.; Cinquini, M.; Colonna, S.; Fornasier, R. *Synthesis* **1974**, 425. Kwart, G.; Evans, E. R. *J. Org. Chem.* **1966**, *31*, 410. (f) Ellis, L. M.; Reid, E. E. *J. Am. Chem. Soc.* **1932**, *54*, 1674. (g) Pan, H.; Fletcher, T. L. *Chem. Ind.* **1968**, 546. (h) Yamada, M.; Sotoya, K.; Sakakibara, T.; Takamoto, T.; Sudoh, R. *J. Org. Chem.* **1977**, *42*, 2180. (i) Vasil'tsov, A. M.; Trofimov, B. A.; Amosova, S. V. *Zh. Organich. Khim.* **1983**, *19*, 1339. (j) Sandler, S. R.; Karo, W. In *Organic Functional Group Preparations*; New York: Academic Press, 1983, 585. (k) Koval, I. V. *Russ. Chem. Rev.* **1993**, *62*, 769.
34. Martin, D. J.; Greco, C. C. *J. Organic Chem.* **1968**, *33*, 1275.
35. (a) Axen, R.; Porath, J.; Ernback, S. *Nature* **1967**, *214*, 1302. (b) Goetzl, E. J.; Metzger, H. *Biochemistry* **1970**, *9*, 1267. (c) Givol, D.; Weinstein, Y.; Gorecki, M.; Wilchek, M. *Biochem. Biophys. Res. Comm.* **1970**, *38*, 825. (d) March, S. C.; Parikh, I.; Cuatrecasas, P. *Anal. Biochem.* **1974**, *60*, 149.
36. Grassetti, D. R.; Murray, J. S. *Arch. Biochem. Biophys.* **1967**, *119*, 41.
37. (a) Eisen, H. N.; Little, J. R.; Osterland, K.; Simms, E. S. *Cold Spring Harbor Symp. quant. Biol.* **1967**, *32*, 75. (b) Eisen, H. N.; Simms, E. S.; Potter, M. *Biochemistry* **1968**, *7*, 4126. (c) Underdown, B. J.; Simms, E. S.; Eisen, H. N. *Biochemistry* **1971**, *10*, 4359.
38. Jencks, W. P.; Gilchrist, M. *J. Am. Chem. Soc.* **1968**, *90*, 2622.
39. Weast, R. C., Ed. *CRC Handbook of Chemistry and Physics*, 68th ed. CRC Press: Boca Raton, 1987-1988, D-162.
40. Jencks, W. P. *Catalysis in Chemistry and Enzymology*, 1st ed.; McGraw-Hill: New York, 1969.
41. Carter, P.; Wells, J. A. *Nature* **1988**, *332*, 564.
42. (a) Stewart, J. D.; Benkovic, S. J. *Nature* **1995**, *375*, 388. (b) Stewart, J. D.; Roberts, V. A.; Thomas, N. R.; Getzoff, E. D.; Benkovic, S. J. *Biochemistry* **1994**, *33*, 1994. (c) Stewart, J. D.; Benkovic, S. J. *Chem. Soc. Rev.* **1993**, 213.
43. (a) Iverson, B. L.; Iverson, S. A.; Roberts, V. A.; Getzoff, E. D.; Tainer, J. A.; Benkovic, S. J.; Lerner, R. A. *Science* **1990**, *249*, 659. (b) Roberts, V. A.;


Iverson, B. L.; Iverson, S. A.; Benkovic, S. J.; Lerner, R. A.; Getzoff, E. D.; Tainer, J. A. *Proc. Natl. Acad. Sci. USA* **1990**, *87*, 6654.

BIOGRAPHICAL SKETCH

Maureen grew up in Alabama where she attended the University of Alabama at Birmingham. In her time at UAB, Maureen studied potential energy surfaces of carbocations with Dr. Koop Lammertsma and also the utilization of β -phosphorothioate nucleotide sugar analogs by glycosyltransferases with Dr. Richard Marchase. She graduated with a B.S. degree in chemistry in 1990.

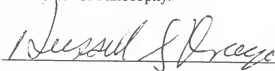
Since enrolling in the University of Florida in the fall of 1990, Ms. Burkart has been studying bioinorganic chemistry under the guidance of Dr. David Richardson. She investigated incorporation of metal complexes into catalytic antibodies. Maureen has accepted a position of visiting assistant professor at Salisbury State University in Maryland where she will teach undergraduate chemistry courses and guide undergraduate research.

I certify that I have read this study and that in my opinion it conforms to acceptable standards of scholarly presentation and is fully adequate, in scope and quality, as a dissertation for the degree of Doctor of Philosophy.



David E. Richardson, Chair
Professor of Chemistry

I certify that I have read this study and that in my opinion it conforms to acceptable standards of scholarly presentation and is fully adequate, in scope and quality, as a dissertation for the degree of Doctor of Philosophy.



Russell S. Drago
Graduate Research Professor of Chemistry

I certify that I have read this study and that in my opinion it conforms to acceptable standards of scholarly presentation and is fully adequate, in scope and quality, as a dissertation for the degree of Doctor of Philosophy.



Martin T. Vala
Professor of Chemistry

I certify that I have read this study and that in my opinion it conforms to acceptable standards of scholarly presentation and is fully adequate, in scope and quality, as a dissertation for the degree of Doctor of Philosophy.



Daniel R. Talham
Associate Professor of Chemistry

I certify that I have read this study and that in my opinion it conforms to acceptable standards of scholarly presentation and is fully adequate, in scope and quality, as a dissertation for the degree of Doctor of Philosophy.

A handwritten signature in cursive script, reading "Paul A. Klein", written in dark ink. The signature is fluid and elegant, with a long horizontal stroke extending to the right.

Paul A. Klein
Professor of Pathology and Laboratory
Medicine

This dissertation was submitted to the Graduate Faculty of the Department of Chemistry in the College of Liberal Arts and Sciences and to the Graduate School and was accepted as partial fulfillment of the requirements for the degree of Doctor of Philosophy.

December 1995

Dean, Graduate School